Doming in compressional orogenic settings: New geochronological constraints from the NW Himalaya

Martin Robyr,[1] Bradley R. Hacker,[2] and James M. Mattinson[2]

Received 3 December 2004; revised 9 December 2005; accepted 18 January 2006; published 1 April 2006.

[1] In the central and southeastern parts of the Himalayas, the High Himalayan Crystalline (HHC) high-grade rocks are mainly exhumed in the frontal part of the range, as a consequence of a tectonic exhumation controlled by combined thrusting along the Main Central Thrust (MCT) and extension along the South Tibetan Detachment System (STDS). In the NW Himalaya, however, the hanging wall of the MCT in the frontal part of the range consists mainly of low- to medium-grade metasediments (Chamba zone), whereas most of the amphibolite facies to migmatitic gneisses of the HHC of Zanskar are exposed in a more internal part of the orogen as a large-scale dome structure referred to as the Gianbul dome. This Gianbul dome is cored by migmatitic paragneisses formed at peak conditions of 800°C and 8 kbar. This migmatitic core is symmetrically surrounded by rocks of the sillimanite, kyanite ± staurolite, garnet, biotite, and chlorite mineral zones. The structural data from the Miyar-Gianbul Valley section reveal that the Gianbul dome is bounded by two major converging thrust zones, the Miyar Thrust Zone and the Zanskar Thrust Zone, which were reactivated as ductile zones of extension referred to as the Khanjar Shear Zone (KSZ) and the Zanskar Shear Zone (ZSZ), respectively. Geochronological dating of monazites from various migmatites and leucogranite in the core of the Gianbul dome indicates ages between 26.6 and 19.8 Ma. These results likely reflect a high-temperature stage of the exhumation history of the HHC of Zanskar and consequently constrain the onset of extension along both the ZSZ and the KSZ to start shortly before 26.6 Ma. Several recent models interpret that ductile extrusion of the high-grade, low-viscosity migmatites of HHC reflects combined extension along the ZSZ and thrusting along the MCT. Hence our new data constrain the onset of the thrusting along the MCT to start shortly before 26.6 Ma. **Citation:** Robyr, M., B. R. Hacker, and J. M. Mattinson (2006), Doming in compressional orogenic settings: New geochronological constraints from the NW Himalaya, *Tectonics*, *25*, TC2007, doi:10.1029/2004TC001774.

1. Introduction

[2] Since the onset of the continental collision at circa 50–55 Ma [*Patriat and Achache*, 1984; *Garzanti et al.*, 1987; *Rowley*, 1996] or even 15 Myr earlier [*Yin and Harrison*, 2000], ~1800–2500 km crustal shortening has occurred between the Indian and Eurasian plates. One third to one half of this contraction was accommodated by shortening within the Indian continental crust [*Molnar and Tapponier*, 1975; *Hodges*, 2000] mainly along SW directed thrust faults that divide the Himalaya into several subparallel tectonic units. One of these units, the High Himalayan Crystalline (HHC), is a 5–10 km thick sequence of amphibolite-facies to migmatitic paragneiss, and constitutes the metamorphic core of the Himalayan orogen (Figures 1 and 2a). This high-grade metamorphic core was thrust southward over the low- to medium-grade sedimentary series of the Lesser Himalaya along the Main Central Thrust (MCT). Several studies indicate that this major intracontinental thrust developed within the Indian margin during the early Miocene, since circa 23 Ma [e.g., *Frank et al.*, 1977; *Hubbard and Harrison*, 1989; *Coleman*, 1998] (Figures 1 and 2a). Broadly contemporaneous movement along the extensional South Tibetan Detachment System [*Burchfiel et al.*, 1992; *Hodges et al.*, 1996; *Coleman*, 1998; *Guillot et al.*, 1994; *Harrison et al.*, 1995; *Dèzes et al.*, 1999] at the top of this metamorphic core zone strongly suggests a tectonically controlled extrusion of the HHC toward the SW. This rather simple geometry fits with most of the investigated sections along the 2500 km length of the Himalayan orogen. Nevertheless, in the northwestern Indian Himalaya, the geologic structure and metamorphic zonation contrast significantly with that in the central and eastern part of the range where the South Tibetan Detachment System is well defined. Indeed, one of the characteristics of the northwestern part of the Indian Himalaya is a gradual decrease in metamorphic grade southwestward. Between the Kulu Valley and the lower Chenab Valley, the MCT juxtaposes two metasedimentary tectonic units of low to medium grade (Figure 1). In this region, the hanging wall of the MCT mainly consists of the greenschist-facies metasediments of the Chamba Zone. In contrast, the higher-grade rocks of the High Himalayan Crystalline Zone (HHCZ) are exposed in a more internal part of the range as a large-scale dome called the Gianbul dome (Figure 2b) [*Dèzes*, 1999; *Steck et al.*, 1999; *Robyr et al.*, 2002]. Farther to the NE, the contact between the HHCZ and the low-grade sediments of the Tethyan Himalaya

[1]Institut de Minéralogie et Géochimie, Université de Lausanne, Lausanne, Switzerland.
[2]Geological Sciences, University of California, Santa Barbara, California, USA.

0278-7407/06/2004TC001774

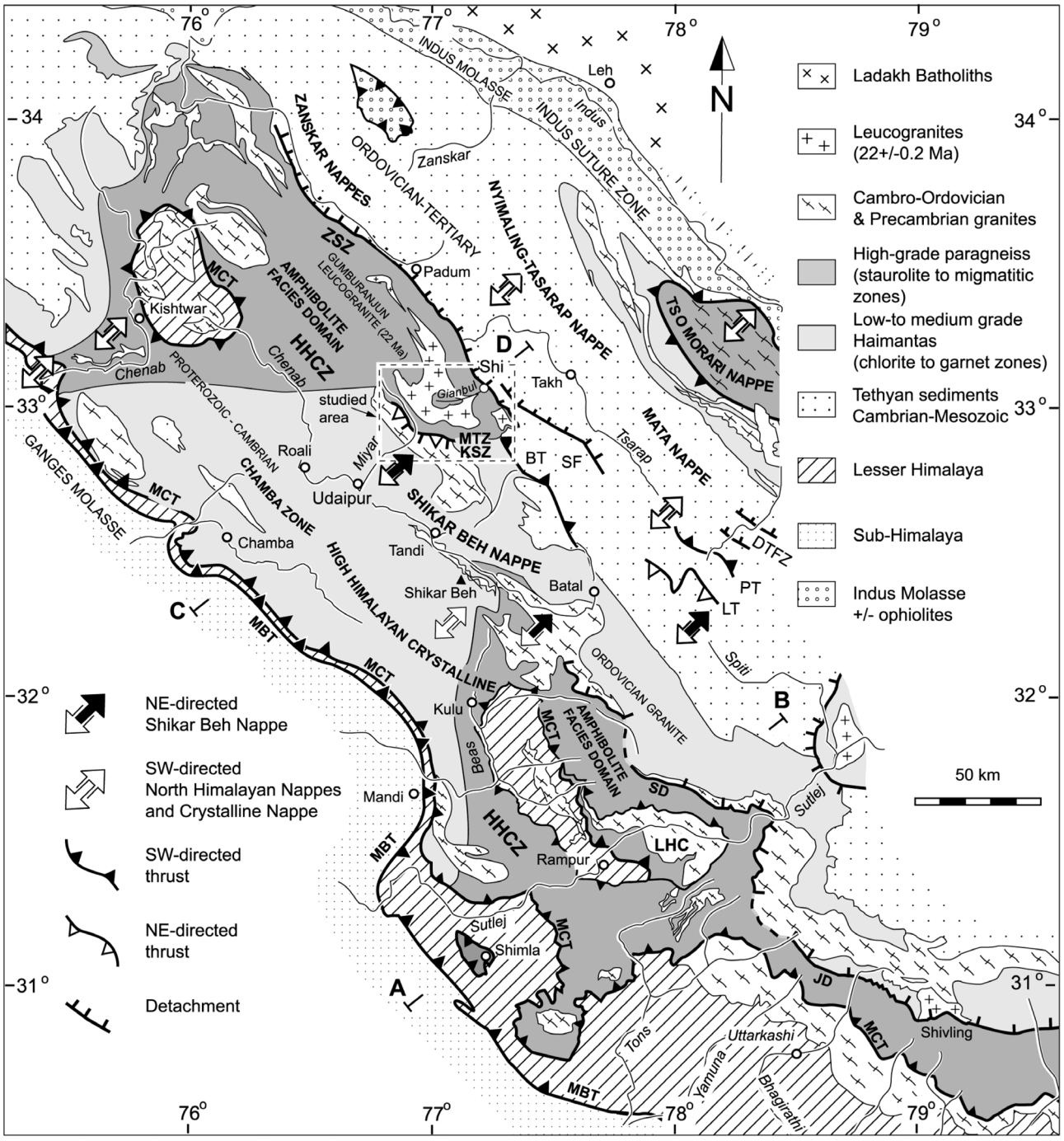

Figure 1. Geological map of the NW Indian Himalaya compiled after *Steck et al.* [1999], *Vannay and Grasemann* [2001], and *Robyr et al.* [2002]. BT, Baralacha La Thrust; DTFZ, Dutung-Thaktote Fault Zone; HHCZ, High Himalayan Crystalline Zone; JD, Jahla Detachment; KSZ, Khanjar Shear Zone; LHC, Lesser Himalayan Crystalline; LT, Lagudarsi La Thrust; MBT, Main Boundary Thrust; MCT, Main Central Thrust; MTZ, Miyar Thrust; PT, Parang Thrust; SD, Sangla Detachment; SF, Sarchu Fault; ZSZ, Zanskar Shear Zone.

corresponds to the 150-km-long Zanskar Shear Zone (ZSZ). This NE dipping extensional shear zone, a local equivalent of the South Tibetan Detachment System, accommodated >35 km slip during the early Miocene [*Dèzes et al.*, 1999; *Dèzes*, 1999]. Since the description of this spectacular tectonic setting by *Herren* [1987], most geological studies have been focused on the north-east border and central part of the HHCZ of Zanskar. As

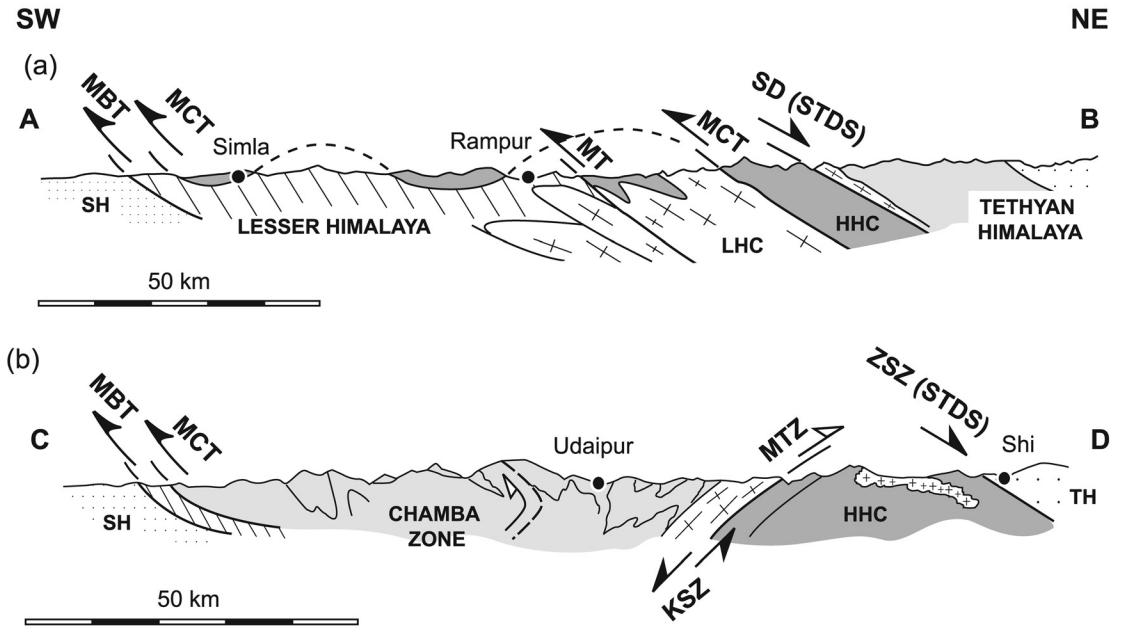

Figure 2. (a) Geological cross section for the Sutlej Valley after *Vannay and Grasemann* [2001]. (b) General cross section for the NW Indian Himalaya across the Gianbul dome along the Miyar Valley–Gianbul Valley section after *Steck et al.* [1999]. Abbreviation and symbols are as in Figure 1.

a consequence, the tectonometamorphic evolution of this part of the range is well constrained [e.g., *Honegger et al.*, 1982; *Kündig*, 1989; *Stäubli*, 1989; *Patel et al.*, 1993; *Dèzes*, 1999; *Searle et al.*, 1999; *Walker et al.*, 1999; *Stephenson et al.*, 2000; *Epard and Steck*, 2004]. In contrast, the timing of the metamorphic and tectonic evolution of the southern limb of the Gianbul dome is still poorly constrained.

[3] This study provides new geochronological data on the tectonometamorphic evolution of the southeastern HHCZ of Zanskar. Together with comparable data from the NE limit of the HHC, these new results allow a time-constrained reconstruction of the tectonometamorphic evolution of this zone across the entire Gianbul dome.

2. Tectonic Setting of the Gianbul Dome Area

[4] The high-grade metamorphic rocks of the HHCZ of Zanskar are exposed as a large-scale dome structure along the Miyar and Gianbul valleys in NW Indian Himalaya (Figures 1 and 3). The geological setting of this Gianbul dome is summarized in the next section, whereas a more detailed account is given by *Robyr et al.* [2002].

[5] The Gianbul dome is cored by migmatitic paragneiss formed at peak conditions of 800°C and 8 kbar. This migmatitic core is symmetrically surrounded by rocks of the sillimanite, kyanite ± staurolite, garnet, biotite, and chlorite mineral zones (Figure 3). The structural and metamorphic data from the Miyar-Gianbul Valley section reveal that the tectonometamorphic evolution of the HHCZ in SE Zanskar is associated with a polyphase tectonic history involving converging nappe structures superimposed by opposite-directed extensional structures (Figure 4) [*Thakur*, 1998; *Dèzes et al.*, 1999; *Steck et al.*, 1999; *Robyr et al.*, 2002]. The first tectonic event corresponds to an early phase of crustal thickening related to NE directed movements. This phase most likely took place during Early to Middle Eocene, and led to the creation of the Shikar Beh nappe, thrusting toward the NE along the Miyar Thrust [*Pognante et al.*, 1990; *Thakur*, 1998]. It is also responsible for the prograde metamorphic field gradient (M1) in the southern limb of the dome [*Steck et al.*, 1999; *Robyr et al.*, 2002]. Beneath the Miyar Thrust, partial melting, related to this initial phase, occurred at temperatures between 750° and 850°C. In the northern limb of the dome, the Barrovian prograde metamorphism is the consequence of a second tectonic phase, associated with the SW directed thrusting of the Nyimaling-Tsarap nappe [*Steck et al.*, 1993]. During this phase, some of the paragneiss were migmatized as a consequence of temperatures up to ~800°C at depth down to ~40 km [*Dèzes et al.*, 1999]. Following these crustal thickening events, exhumation and doming of the high-grade metamorphic rocks of the HHCZ were controlled by extension along the north dipping ZSZ, in the frontal part of the Nyimaling-Tsarap nappe, as well as by extension along the south dipping Khanjar Shear Zone (KSZ), in the

Figure 3. Geological and metamorphic map of the Giabul dome area showing the locations of samples analyzed for geochronology (after *Dèzes et al.* [1999], *Robyr et al.* [2002], and original survey by M. Robyr).

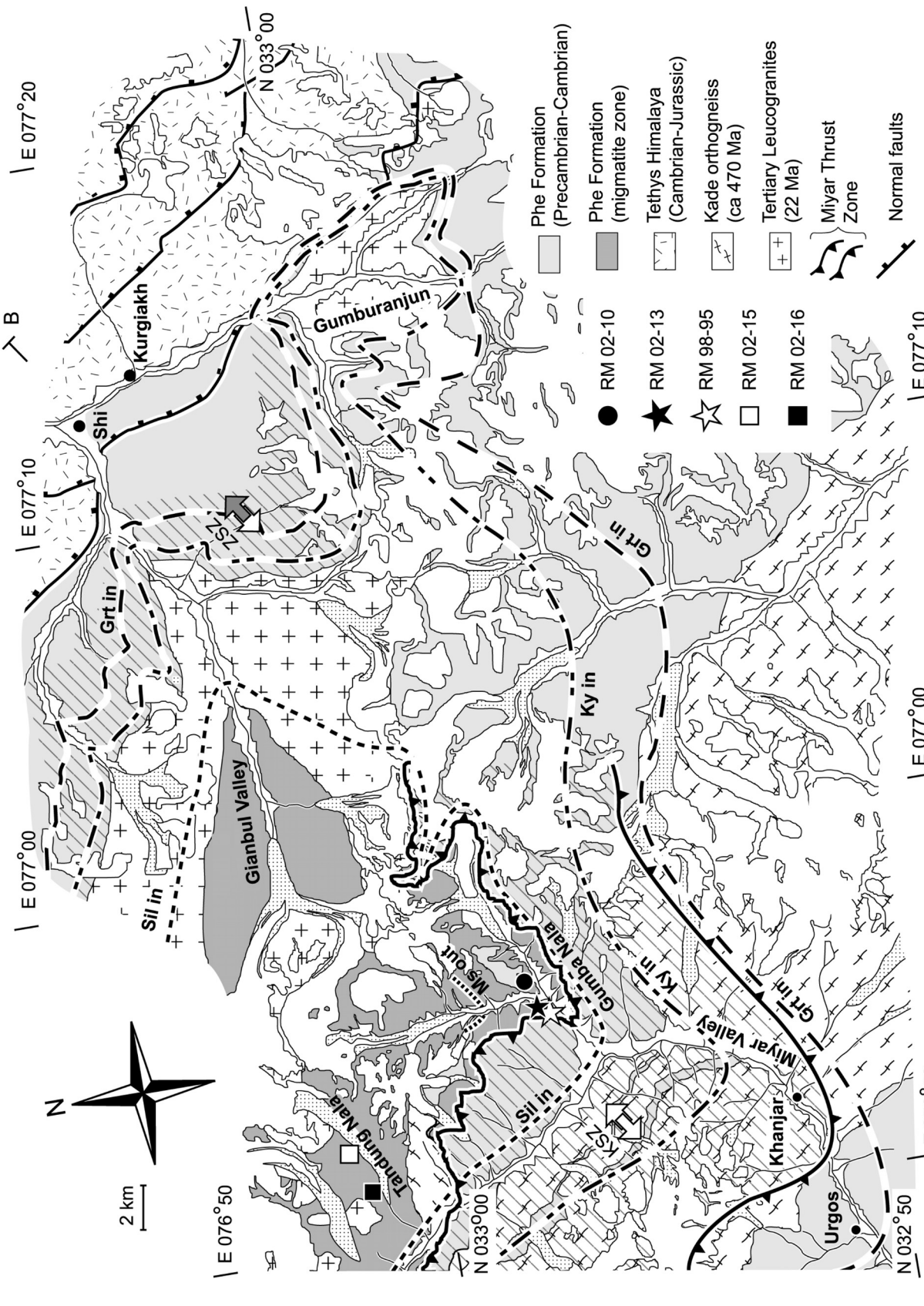
Phe Formation (Precambrian-Cambrian)
Phe Formation (migmatite zone)
Tethys Himalaya (Cambrian-Jurassic)
Kade orthogneiss (ca 470 Ma)
Tertiary Leucogranites (22 Ma)
Miyar Thrust Zone
Normal faults
RM 02-10
RM 02-13
RM 98-95
RM 02-15
RM 02-16
Kurgiakh
Shi
Gumburanjun
Gianbul Valley
Tandung Nala
Gumba Nala
Miyar Valley
Khanjar
Urgos
Grt in
Ky in
Sil in
MS out
KSZ
TSZ
A
B
N
2 km
E 077°20
E 077°10
E 077°00
E 076°50
E 076°50
N 033°00
N 033°00
N 032°50

Figure 3

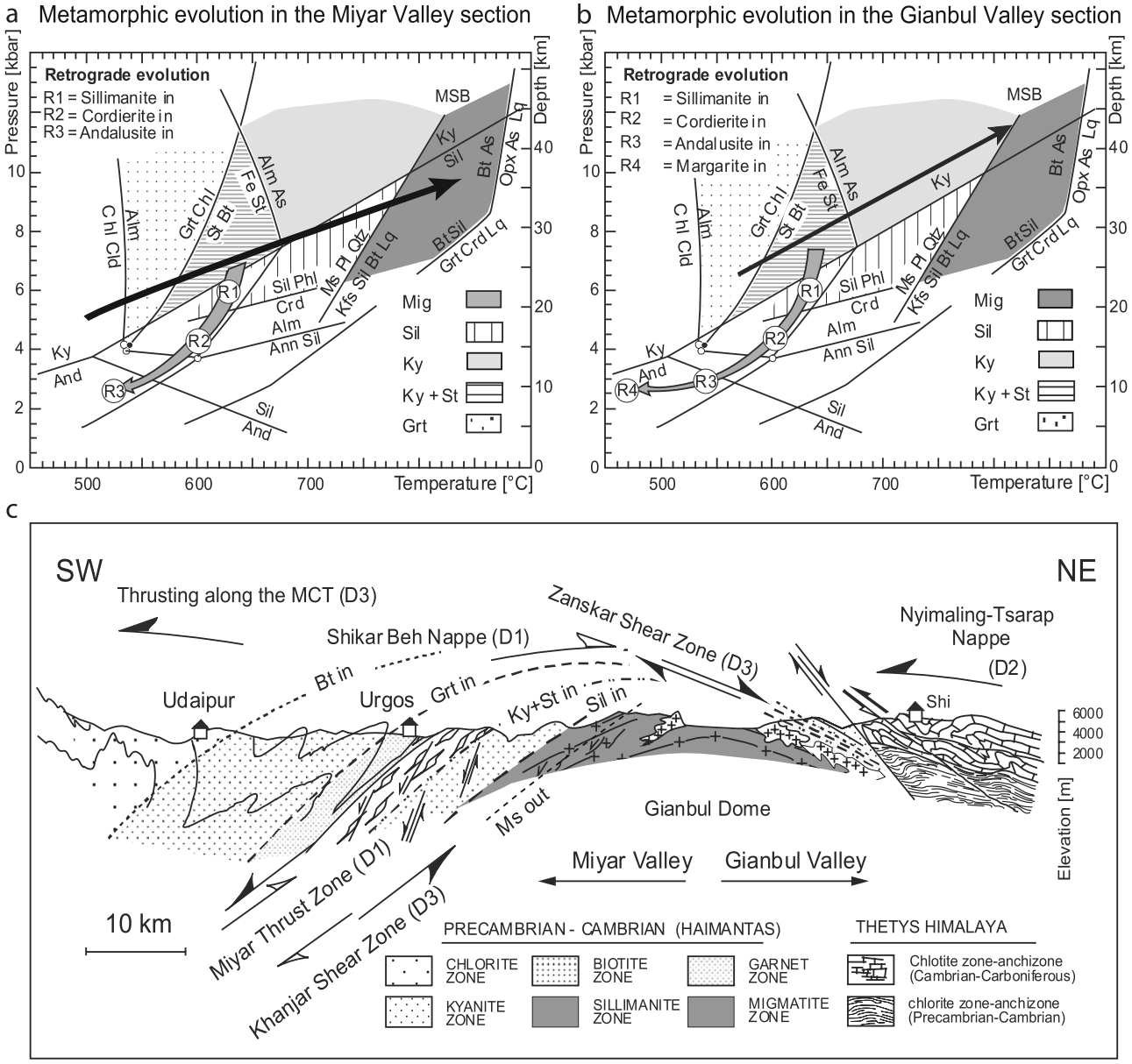

Figure 4. Peak P-T estimates (a) for the HHCZ of the Miyar Valley and (b) for the Gianbul Valley reported in a petrogenetic grid for metapelites. The muscovite dehydration reactions labeled "MBS" correspond to the experimentally determined partial melting conditions for muscovite + biotite bearing Himalayan metapelites, respectively [*Patiño-Douce and Harris*, 1998]. The biotite dehydration melting reaction is taken from *Spear et al.* [1999]. The black arrow represents the prograde metamorphic field gradient in the Miyar and Gianbul valleys. The grey arrow corresponds to the retrograde metamorphic evolution of the kyanite + staurolite zone assemblages, deduced from textural relations (see text). Abbreviations are Alm, almandine; And, andalusite; Ann, annite; As, aluminosilicate; Bt, biotite; Chl, chlorite; Cld, chloritoid; Crd, cordierite; Grt, garnet; Kfs, K-feldspar; Ky, kyanite; Lq, liquid (melt); Ms, muscovite; Opx, orthopyroxene; Phl, phlogopite; Sil, sillimanite; St, staurolite. (c) Geological cross section through the Gianbul dome along the Miyar Valley and Gianbul Valley.

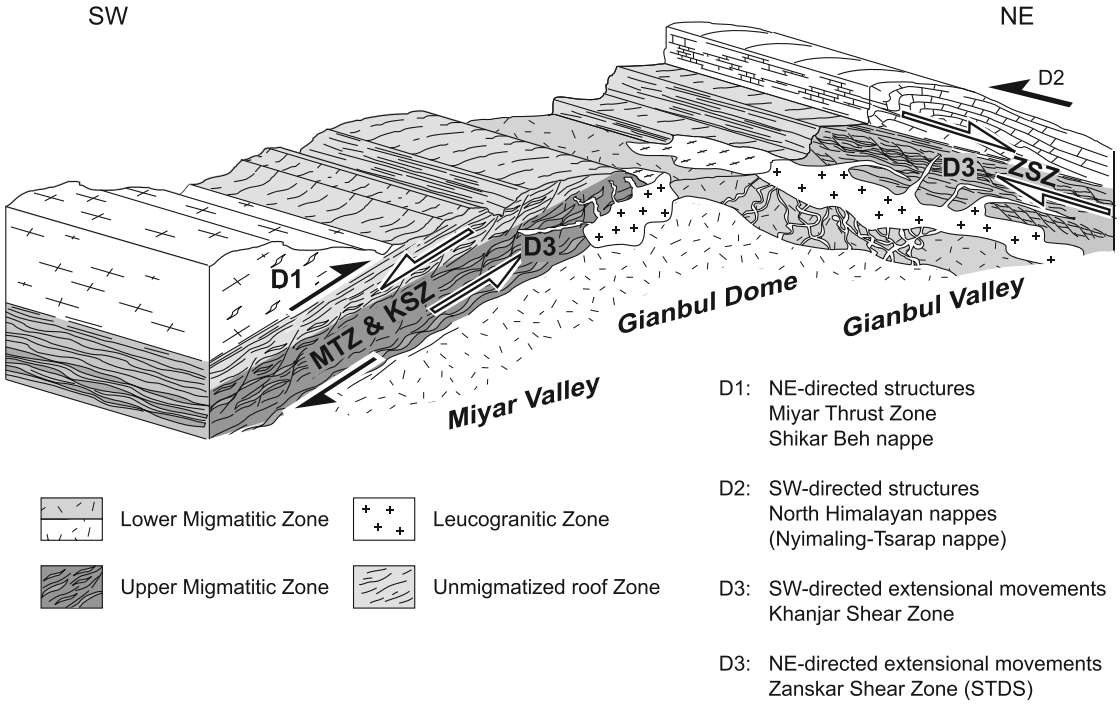

Figure 5. Synthetic block diagram of the Gianbul dome along the Miyar Valley–Gianbul Valley transect. The block diagram resumes the deformation phases in the studied area and shows the structural relationship between migmatites, leucogranites, and dikes.

southern limb of the Gianbul dome. Rapid synconvergence extension along both of these detachments induced a nearly isothermal decompression, resulting in a high-temperature/low-pressure metamorphic overprint.

3. Geological Setting of the Migmatitic–Leucogranitic Complex of the Gianbul Dome Area

[6] The core of the Gianbul dome mainly consists of a migmatitic-leucogranitic intrusive complex, bounded by the SW dipping KSZ to the south [*Steck et al.*, 1998; *Robyr et al.*, 2002; *Robyr*, 2002] and the NE dipping Zankar Shear Zone to the north [*Dèzes*, 1999; *Dèzes et al.*, 1999] (Figures 4 and 5). This leucogranite intrusive complex is critical for understanding the tectonometamorphic evolution of the HHCZ of Zanskar because it records evidence for multiple phases of anatexis related to multiple deformational events.

[7] A first generation of migmatites, referred in this study to as the upper migmatitic zone, is observed in the footwall of the Miyar Thrust Zone and forms the greatest part of the cliff bordering the Gumba Nala section, in the upstream part of the Miyar Valley (Figure 3). Except for the presence of granitic segregations, the overall mineralogy and fabric of the migmatitic paragneiss is very similar to the sillimanite zone and is characterized by the assemblage sillimanite + quartz + biotite + garnet + plagioclase ± muscovite ± K-feldspar. The outer part of the migmatite zone is composed of muscovite-present assemblages, whereas the central part is delimited by a sharp muscovite-out isograd (Figures 3 and 4c) [*Robyr et al.*, 2002]. Thermobarometry plus oxygen isotope thermometry indicate partial melting at temperatures ~800°C and pressures of ~8 kbar [*Robyr et al.*, 2002]. Within this migmatite zone, a clear top-to-the-NE shear sense is indicated by asymmetrical boudinage of leucogranitic layers and pinch-and-swell structures (Figure 6). Moreover, sigmoidal inclusion trails in syntectonic garnet porphyroblasts indicate prograde growth during NE directed shearing. These overall observations indicate that partial melting in the Gumba Nala section occurred in response to crustal thickening related to the NE directed Shikar Beh nappe emplacement. In a late phase of deformation, the NE directed contractional movements were overprinted by SW extension associated with displacement along the Khanjar Shear Zone (Figure 7). Veins of anatectic melt intruding these extensional structures indicate that rapid isothermal decompression associated with this extension produced a second generation of partial melt. In the northernmost part of the Gumba Nala, the migmatites are intruded by a leucogranitic pluton which is likely connected to the early Miocene leucogranitic bodies forming a large part of the HHCZ of SE Zanskar and referred in this region to as the Gumburanjun leucogranites [*Dèzes*, 1999]. Along the Miyar Valley–Gianbul Valley transect, this leucogranitic pluton is characterized by a relatively homogeneous core surrounded by a spectacular network of dikes (Figure 5). At the base of the pluton, the network of dikes is directly rooted into a lower migmatitic zone and converges upward to feed the leucogranitic pluton. Along the Miyar Valley–Gianbul

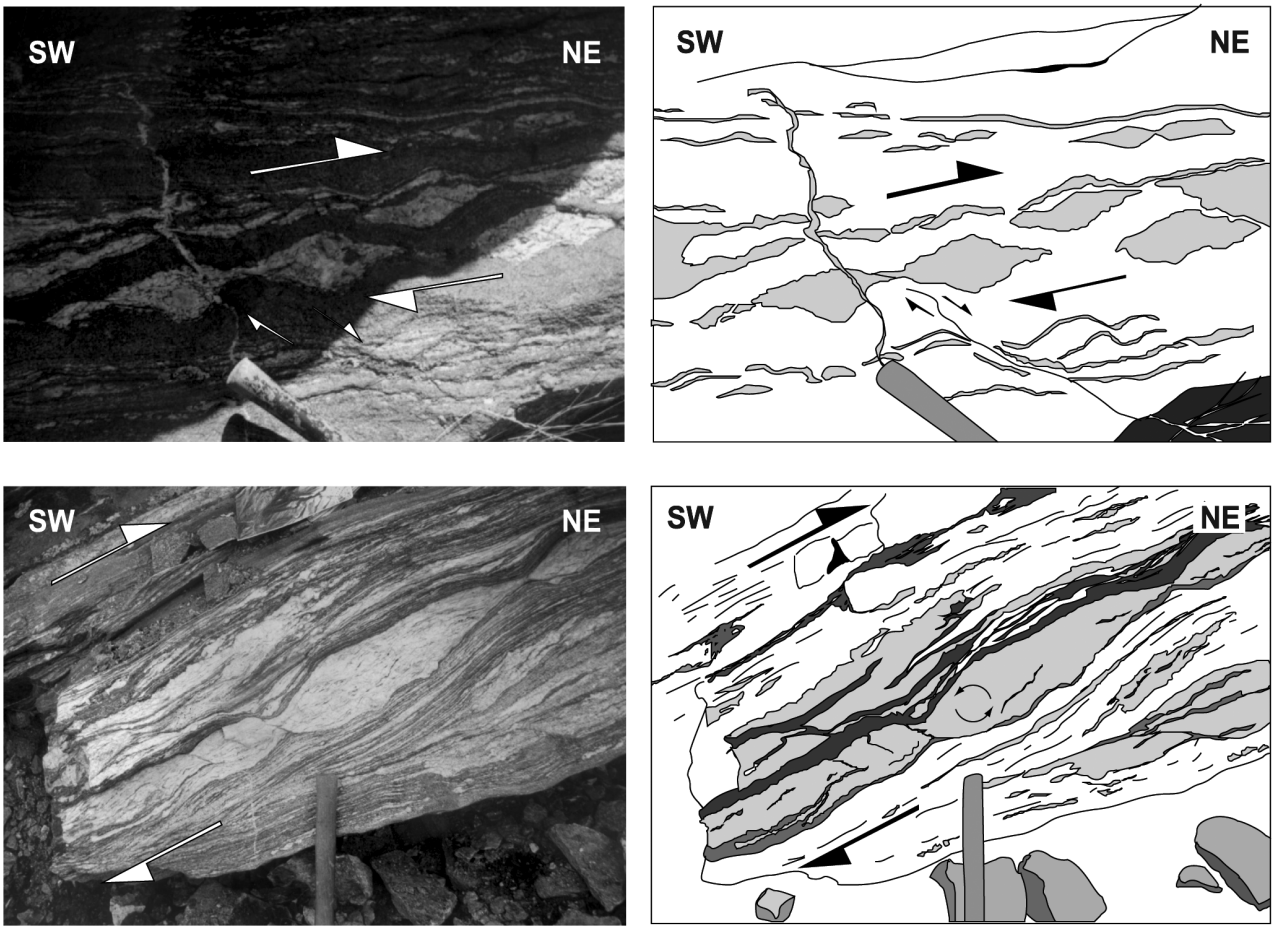

Figure 6. Asymmetrical boudinage of leucogranitic layers and pinch-and-swell structures showing NE directed sense of shearing in the migmatitic zone in the footwall of the Miyar Thrust Zone (Gumba Nala area). Sections are parallel to the stretching lineation and normal to the main foliation.

Valley section, this lower migmatitic zone is restricted to the Gianbul Valley section and constitutes the basal part of the intrusive complex. It consists of migmatitic paragneiss with minor metabasites. Thermobarometry of metabasite lenses within the migmatite indicates peak conditions of ~810°C/12 kbar. P-T data from metapelite samples yield final equilibration at ~580°C/3 kbar [*Dèzes et al.*, 1999] implying that peak conditions were followed by a near-isothermal decompression and a HT/LP metamorphic overprint. It consequently appears that a large part of the partial melting observed on the northern limb of the Gianbul dome may have been triggered by muscovite-dehydration melting during decompression rather than having occurred exclusively during peak Barrovian metamorphism. At the top of the leucogranitic plutons, the network of dikes becomes less dense and intrudes the overlying country rock paragneiss. It consists of kyanite-bearing metasediments on the northern limb of the Gianbul dome, and migmatitic metasediments on the southern limb. In the Gianbul Valley section, most of the leucogranitic dikes were reoriented parallel to the main foliation by SW directed extension along the ZSZ. However, some younger undeformed dikes cut the main foliation and postdate the extension [*Dèzes et al.*, 1999; *Dèzes*, 1999]. On the southern limb of the dome along the Gumba Nala section, undeformed aplitic and pegmatitic leucogranitic dikes crosscut the SW directed extensional structures testifying that, in the SW half of the dome, the dikes intruded the shear zone after ductile motion along the KSZ had stopped.

4. Geochronology

4.1. Previous Age Constraints

[8] Sm–Nd dating of garnet from the northernmost part of the HHCZ of Zanskar indicates metamorphism between 33 and 28 Ma [*Vance and Harris*, 1999]. These ages agree with metamorphic monazite growth ages of 37–29 Ma from the footwall of the ZSZ near the Gumburanjun area [*Walker et al.*, 1999]. The thrust responsible for this crustal thickening must be located between the HHCZ and the Tethyan Himalaya, given that the latter unit is not affected by high-grade metamorphism. Consequently, the high-grade metamorphism in the HHCZ is most likely the consequence of

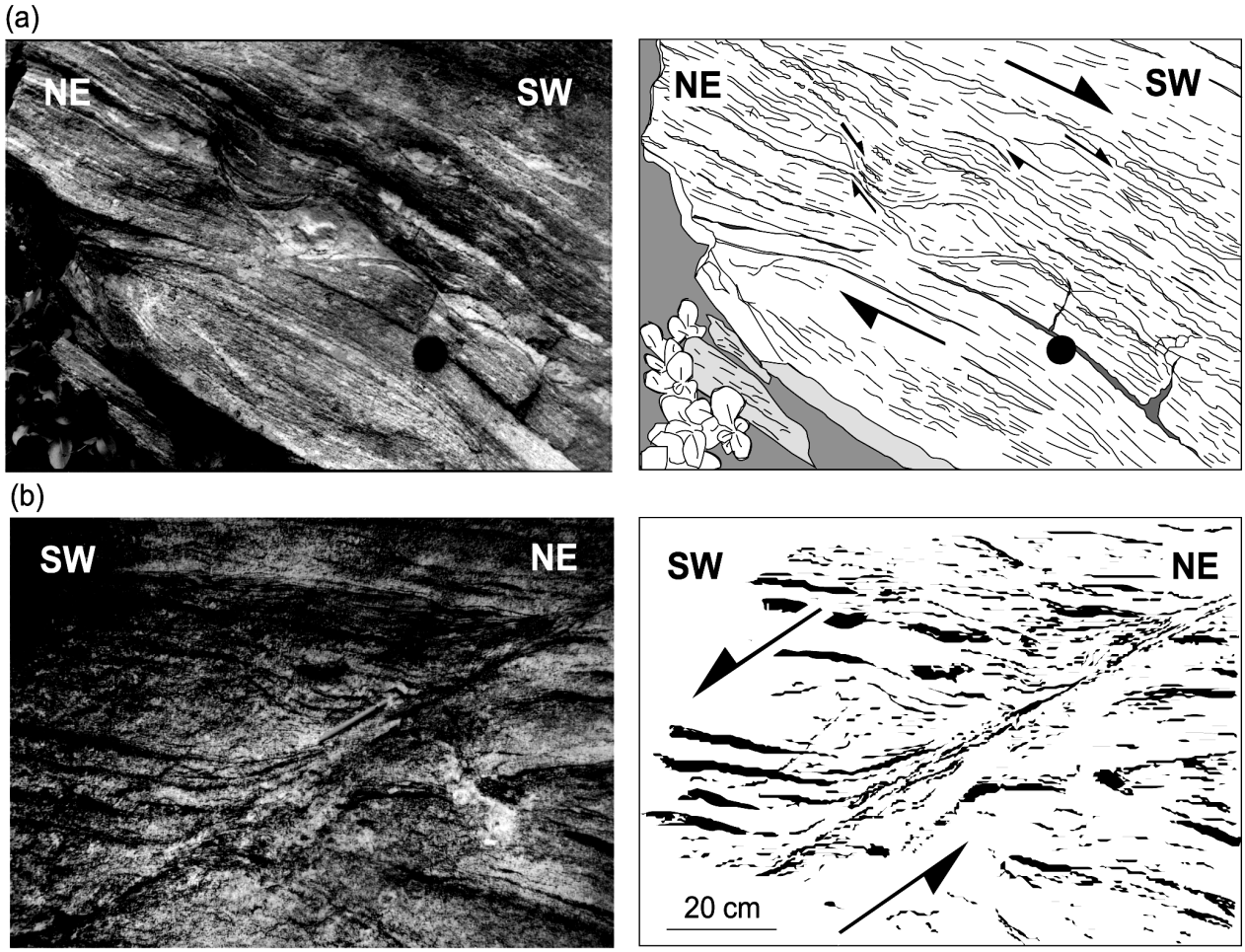

Figure 7. (a) Asymmetrical boudinage of leucogranitic levels in the migmatitic zone indicating a top-to-the-SW ductile extensional shearing along the Khanjar Shear Zone (Gumba Nala area). (b) Asymmetrical extensional shear bands overprinting the main foliation in the paragneiss from the migmatitic zone (Gumba Nala area). Both sections are parallel to the stretching lineation and normal to the main foliation.

the NE directed underthrusting of this unit beneath the Tethyan Himalaya. This event was likely coeval with the SW directed nappe tectonics (e.g., Nyimaling-Tsarap nappe) responsible for the middle Eocene low-grade metamorphism in the Tethyan Himalaya constrained by $^{40}Ar/^{39}Ar$ white mica ages (circa 45–42 Ma [*Bonhomme and Garzanti*, 1991; *Wiesmayr and Grasemann*, 1999; *Schlup et al.*, 2003]). This interpretation is consistent with the observations by *Patel et al.* [1993] that the extensional ZSZ reactivates a former thrust.

[9] Geochronological data from strongly deformed dikes indicate that the main phase of ductile deformation along the ZSZ was ongoing at 22 Ma, and data from undeformed leucogranitic dikes intruding the base of the ZSZ along the Gianbul Valley reveal that motion along the ZSZ ceased before 19.8 Ma. Hence partial melting in the NE half of the Gianbul dome must have occurred in this timeframe [*Dèzes et al.*, 1999]. Partial melting in this part of the Himalayan range is collectively interpreted as the consequence of the rapid exhumation of the high-grade metamorphic rocks along the ZSZ, in good agreement with the isothermal decompression revealed by the P-T data. On the basis of these observations, it is commonly assumed that the onset of extension along the ZSZ was not significantly older than 22 Ma.

[10] In contrast with the tight constraints on the timing of the tectonometamorphic evolution of the NE half of the Gianbul dome, the timing of the crustal thickening and subsequent extension on the southern limb of the dome is not constrained.

4.2. Monazite U-Th-b Age Data

4.2.1. Timing of Crustal Shortening Along the Miyar Thrust Zone

[11] One of the major features of the tectonometamorphic evolution of the HHCZ of the Zanskar–Lahul region is that the earliest phase of metamorphism and tectonism in this portion of the Himalaya relates to NE directed thrusting.

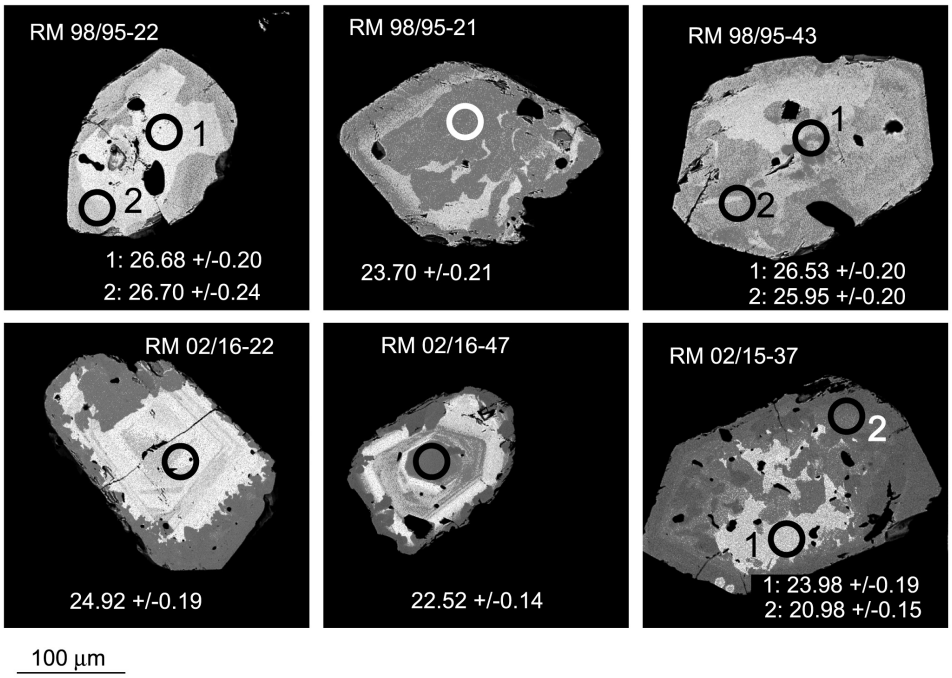

Figure 8. Backscattered electron microprobe images of some of the analyzed monazites illustrating patchy zoning (RM 98/95-21 and RM 02-15) and growing zoning (RM 02/16-22 and 23). Numbered circles indicate areas where age analyses were taken. Note that for the sample RM 98/95, the data are roughly the same wherever is the location of the analyzed spot through the grain.

This NE directed thrusting clearly contrasts with the predominant Himalayan deformation manifested by folding and thrusting toward the SW. Yet NE directed structures have also been observed between the Miyar Valley and the upper Spiti Valley [*Steck et al.*, 1993; *Vannay*, 1993; *Epard et al.*, 1995; *Vannay and Steck*, 1995; *Steck et al.*, 1998, 1999; *Wyss et al.*, 1999; *Robyr et al.*, 2002] (Figure 1). In the Chandra Valley and in the upper Spiti Valley, structural interference patterns demonstrate that the structures associated with the SW directed Tethyan Himalayan Mata nappe overprint those related to NE directed movements. These NE directed structures are collectively interpreted as testifying to an early NE directed crustal thickening associated with the emplacement of the Shikar Beh nappe [*Steck et al.*, 1993, 1999; *Steck*, 2003]. However, no quantitative data constrain the chronology of the tectonometamorphic evolution in the southern part of the dome.

4.2.2. Methodology

[12] To obtain quantitative constraints on the age of the NE directed thrusting, four samples (3–5 kg) were collected from two areas in the northern part of the Miyar Valley, two from the Gumba Nala area (samples RM 98-95 and RM 02-13) and two from the Tandung Nala area (samples RM 02-15 and 02-16; Figure 3). Both exposures are located in the upper migmatitic zone and comprise migmatitic sedimentary rocks intruded by undeformed pegmatite dikes. These migmatitic rocks contain NE directed contractional structures associated with the Miyar Thrust Zone (Figure 7) overprinted by SW directed extensional shear bands of the KSZ. Structural observations and thermobarometric investigations suggest a close genetic relation between the NE directed crustal thickening phase and the leucogranitic melt production.

[13] Isotope dilution thermal ionization mass spectrometry (ID-TIMS) and secondary ion mass spectrometry (SIMS) were used to constrain the timing of contraction along the Miyar Thrust Zone. Single grains of clear, crack-free monazite and xenotime were handpicked from concentrates isolated using conventional heavy liquid and magnetic separation techniques. Backscattered electrons (BSE) were used to image the internal structures of the monazite grains. The BSE images (Figure 8) highlight two different types of zoning in the monazites: (1) concentric zoning interpreted as a growth zoning; (2) so-called patchy zoning [*Ayers et al.*, 1999]. This patchy zoning is characterized by irregularly shaped zones that overprint preexisting concentric zoning; it is interpreted as resulting from recrystallization of preexisting monazite [*Poitrasson et al.*, 1996; *Hawkins and Bowring*, 1997; *Ayers et al.*, 1999]. This interpretation is supported by the systematically younger ages measured on the monazites that show patchy zoning (Figure 8). As the aim of this study is to constrain the timing of the earliest phase of metamorphism and tectonic related to NE directed thrusting, the ages from the patchy zoned monazites are not considered here.

4.2.3. Results

[14] Monazite and xenotime extracted from samples RM 98-95 and RM 02-13 were analyzed using ID-TIMS at the

Table 1. TIMS Results for Monazite and Xenotime[a]

Sample	Weight, mg	^{238}U, ppm	Measured Isotopic Ratios[b]			Calculated Ratios[c]			Calculated Ages in Ma ± (2-sigma Ma Errors)[d]		
			^{208}Pb/^{206}Pb	^{207}Pb/^{206}Pb	^{204}Pb/^{206}Pb	^{206}Pb*/^{238}U	^{207}Pb*/^{235}U	^{207}Pb*/^{206}Pb*	^{206}Pb*/^{238}U	^{207}Pb*/^{235}U	^{207}Pb*/^{206}Pb*
RM02-10 mon	1.5	8194	2.3587	0.060516	0.001063	0.0036341	0.022462	0.044829	23.38 (0.05)	22.56 (0.19)	minus 65 (20)
RM98-95 mon	1.5	2887	1.8749	0.060535	0.000984	0.0040652	0.025803	0.046036	26.15 (0.05)	25.87 (0.20)	minus 0.5 (19)
RM02-13 mon	1.4	2519	1.4558	0.058155	0.0004397	0.007599	0.054188	0.051721	48.80 (0.10)	53.58 (0.17)	273.1 (7.8)
RM02-13 xen	1.3	8644	0.05741	0.053333	0.0004491	0.0034113	0.021975	0.046721	21.95 (0.04)	22.07 (0.08)	35.0 (8.4)
RM02-13 xen*									22.04 (0.04)	22.07 (0.08)	25.6 (8.4)

[a]Asterisk indicates ages corrected for 80% ^{230}Th deficiency.
[b]Measured isotopic ratios, corrected for 0.12%/amu mass fractionation and 205Pb spike composition.
[c]Corrected for common Pb using 206/204 = 18.70, 207/204 = 15.60.
[d]Ages calculated using decay constants of *Jaffey et al.* [1971]. Errors estimated from analytical errors and uncertainty in common Pb corrections.

University of California, Santa Barbara (Table 1). Xenotime sample RM 02-13 gave concordant ages of 22.07 ± 0.08 Ma and monazites from the same sample yielded a ^{235}U/^{207}Pb age of 53.58 ± 0.17 Ma and a ^{207}Pb/^{206}Pb age of circa 273 Ma. This inconsistency unequivocally indicates the presence of an inherited component. Monazites from sample RM 98-95 gave concordant ages of 25.87 ± 0.20 Ma.

[15] To separate the inherited and younger components, monazites from three samples (RM 98-95, RM 02-15, and RM 02-16) from the migmatitic zone were analyzed by SIMS at the University of California, Los Angeles following the analytical procedures of *Harrison et al.* [1995, 1999]. The measured ^{232}Th/^{208}Pb ages vary from 27–22 Ma (Table 2 and Figure 9). The results obtained from sample RM 98-95 are remarkably consistent, yielding a mean age of 26.58 ± 0.21 Ma (Figures 8 and 9). Other samples gave more scattered ages between 25 and 22 Ma.

4.2.4. Interpretation

[16] Several recent studies revealed that interpreting monazite ages can be challenging [*Foster et al.*, 2000; *Catlos et al.*, 2002; *Hawkins and Bowring*, 1999] notably due to the growth and recrystallization of monazite during prograde and retrograde metamorphism [*Lanzirotti and Hanson*, 1996; *Fitzsimons et al.*, 1997; *Hawkins and Bowring*, 1997; *Townsend et al.*, 2001]. One of the major problem is estimating the closure temperature of Pb in monazite. Recent work by *Smith and Giletti* [1997] and by *Cherniak et al.* [2004] attempted to resolve this issue. In a ion microprobe depth profiling study, *Smith and Giletti* [1997] measured Pb tracer diffusion in natural monazite, determining an activation energy of 43 ± 11 kcal/mol. *Cherniak et al.* [2004] reported an activation energy over three times higher (E = 149 ± 9 kcal/mol and D_o = 0.94 m^2/s) based on a combined Rutherford backscattering and ion microprobe study of synthetic monazite. The high value reported by *Cherniak et al.* [2004] suggests that the concept of closure temperature is largely irrelevant for the U-Th-Pb monazite system under crustal conditions as Pb is predicted to be essentially immobile [*Harrison et al.*, 2002]. Indeed, most recent studies estimate closure temperatures of 700–800°C [*Copeland et al.*, 1988; *Parrish*, 1990; *Suzuki et al.*, 1994; *Braun et al.*, 1998; *Kamber et al.*, 1998], bearing in mind that closure temperature depends on grain size and cooling rate.

[17] The Th-Pb age range recorded in the studied monazites leads to three possible interpretations.

[18] 1. As cited above, structural relationships reveal that the NE directed crustal thickening phase was followed by contraction related to the southwestward emplacement of the Nyimaling-Tsarap nappe. Geochronological data reveal that the latter ranged from the middle Eocene to the late Oligocene [*Vance and Harris*, 1999; *Walker et al.*, 1999; *Schlup et al.*, 2003]; therefore the NE directed Shikar Beh nappe emplacement must be older than middle Eocene. Our monazite ages therefore cannot correspond to the peak metamorphic conditions recorded in the migmatitic zone of the Miyar Valley section. The monazites analyzed in this study are ~200 μm in diameter, and some reach 400 μm. If the experimental data of *Smith and Giletti* [1997] are

Table 2. Monazite Ion Microprobe Ages

Gumba Nala				Tandung Nala			
RM 98-95[a]		RM 02-10[b]		RM 02-15[a]		RM 02-16[a]	
Grain-Spot[c]	Age,[d] Ma	Grain-Spot[c]	Age,[d] Ma	Grain-Spot[c]	Age,[d] Ma	Grain-Spot[c]	Age,[d] Ma
14-1	26.82 (0.22)	5-1	22.93 (0.27)	7-1	24.21 (0.19)	2-1	24.29 (0.21)
18-1	26.34 (0.34)	23-1	22.46 (0.23)	11-1	22.2 (0.15)	5-1	22.28 (0.19)
22-1	26.68 (0.20)	23-2	19.92 (0.42)	23-1	25.57 (0.37)	17-1	22.86 (0.18)
22-2	26.7 (0.24)	24-1	22.88 (0.27)	24-1	23.3 (0.19)	22-1	24.92 (0.19)
24-1	26.89 (0.19)	24-2	23.37 (0.79)	30-1	22.88 (0.16)	23-1	22.52 (0.17)
35-1	27.02 (0.25)	25-1	23.56 (0.33)	30-2	22.32 (0.17)	27-1	25.36 (0.23)
37-1	26.6 (0.21)	27-1	23.64 (0.39)	37-1	23.98 (0.19)	34-1	23.45 (0.17)
38-1	26.36 (0.19)			37-2	20.98 (0.15)	47-1	22.52 (0.14)
40-1	26.7 (0.20)			38-1	21.9 (0.19)		
43-1	26.53 (0.20)						
43-2	25.95 (0.20)						

[a]Migmatite sample.
[b]Undeformed leucogranitic dikes.
[c]The nomenclature indicates the grain and spot of the analyzed monazite.
[d]Spot age (±1σ).

correct, a 150 μm diameter monazite heated to 800°C for 10 Myr will lose ~100% of its Pb, whereas a 200 μm diameter large monazite will lose ~90% of its Pb. In this case, the monazite ages that are so much younger than the NE directed faulting could be explained by Pb loss during the M1 thermal event. As a consequence, these ages would most likely reflect part of the exhumation history of these migmatites, and indicate that these high-grade metamorphic rocks cooled below closure to monazite Pb loss between 26.6 Ma and 22 Ma.

[19] 2. According to *Cherniak et al.* [2004], Pb is nearly immobile in monazite at crustal temperatures and each

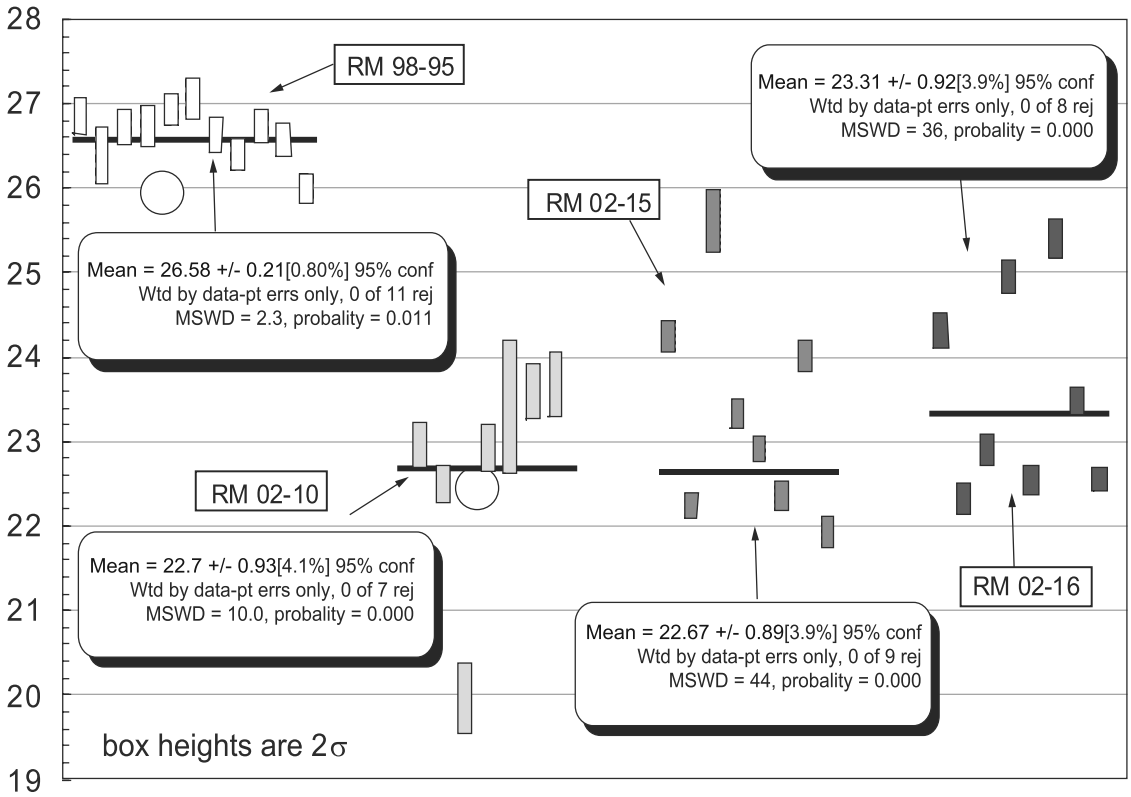

Figure 9. A weighted average plot of $^{232}Th-^{208}Pb$ age of analyzed monazites. Errors bars on the $^{232}Th-^{208}Pb$ age are 2σ. The two large white dots refer to the ID-TIMS U-Pb preliminary results.

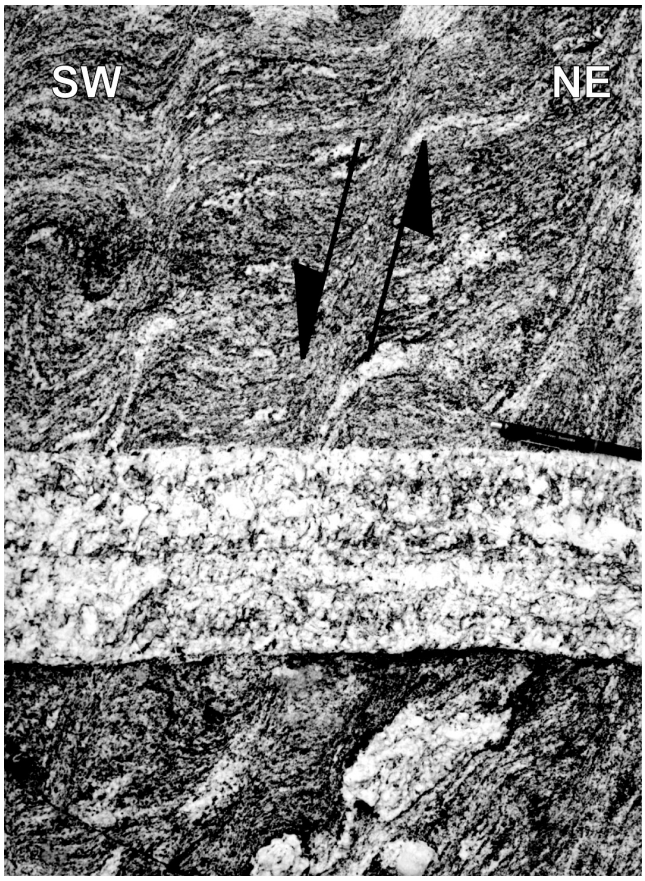

Figure 10. Undeformed pegmatitic dike crosscutting the SW directed extensional shear bands of the Khanjar Shear Zone (Gumba Nala area).

datum represents exactly the (re)crystallization age. As a consequence, our monazite ages cannot correspond to the NE directed crustal thickening phase and require a second episode of monazite growth or recrystallization, following the M1 peak metamorphism recorded in the migmatites of the Miyar Valley. Field evidence indicates two phases of anatexis in this valley. Indeed, the migmatitic rocks yield NE directed contractional structures overprinted by SW directed extensional shear bands. Veins of anatectic melt intruding these extensional structures indicate that near-isothermal decompression associated with this extension produced a second generation of melt. Monazite may dissolve into silicate melt and recrystallize on melt solidification [*Hawkins and Bowring*, 1999; *Rubatto et al.*, 2001; *Pyle et al.*, 2001]. It consequently appears that our monazite ages most likely reflect a second stage of monazite crystallization associated with the exhumation-controlled partial melting along the SW dipping extensional KSZ.

[20] 3. Dissolution and reprecipitation of monazite can be caused by hydrothermal fluid infiltration during retrogression [*Ayers et al.*, 1999]. A second generation of idioblastic new monazite can grow during the retrograde ductile deformation of Barrovian metamorphic rocks that contain small, xenoblastic, prograde monazite [*Lanzirotti and Hanson*, 1996]. Such an interpretation is consistent with the geological characteristics of the upstream part of Miyar Valley where not only the presence of an extensional shear zone but also the production of a second generation of migmatites could drive the growth and crystallization of new monazites. This interpretation suggests that the monazites we dated result from retrograde metamorphism. The absence of older monazites could be explained by our focus on large, clear, crack-free, idioblastic monazites.

[21] Considering the diffusion parameters for Pb and the relatively large grain size of the investigated monazites (up to 300–400 μm), it seems unlikely to us that Pb loss alone can account for the homogeneous late Oligocene ages measured from core to rim (e.g., RM 98/95-43; Figure 8). Consequently, we interpret the late Oligocene ages as reflecting crystallization of new monazite during retrogression. In any case, the measured monazite ages do not reflect peak metamorphic conditions following NE directed thrusting (Miyar Thrust) and we interpret them to date a high-temperature stage of the exhumation history of the Gianbul dome.

4.2.5. Timing of Extensional Shearing Along the Khanjar Shear Zone

[22] The extensional KSZ represents one of the many shear zones within the Himalaya that show that major extensional structures were active at the same time as major contractional structures (e.g., the South Tibetan Detachment System [*Hodges et al.*, 1992] and the Karcham Normal Fault [*Janda et al.*, 2002]). In the southern limb of the Gianbul dome, SW directed extension along the KSZ sheared the M1 isograds and dropped the low-grade Chamba Zone down against the high-grade HHCZ of Zanskar. In the footwall of the KSZ, petrographic investigations indicate a retrograde evolution characterizing a nearly isothermal decompression.

[23] Our new SIMS ages of monazites from migmatites in the footwall of the KSZ indicate that these rocks were exhumed between 26.6 and 23 Ma; the onset of extension along the KSZ is thus constrained to shortly before 26.6 Ma. To date the end of movement along the KSZ, we performed ID-TIMS analyses on monazites extracted from an undeformed leucogranitic dike (RM 02-10) that cuts across the extensional structures of the KSZ (Table 1 and Figure 10). The resulting U and Pb ratios are concordant and indicate an age of 22.56 ± 0.19 Ma. SIMS of monazites from the same sample gave ages from 23.6 Ma to 19.9 Ma (Table 2 and Figure 9) in agreement with the ID-TIMS results. These ages are consistently younger than the migmatite ages reported above, and equivalent to U-Pb ages from leucogranitic plutons (22.2 ± 02 Ma [*Dèzes et al.*, 1999]) cropping out on the northern limb of the Gianbul dome in the Gianbul Valley. These results strongly suggest that these undeformed leucogranitic dikes and small plutons exposed in the upstream part of the Miyar Valley are associated with the intrusion of the early Miocene Gumburanjun Leucogranite a few kilometers to the north. Hence our new results indicate

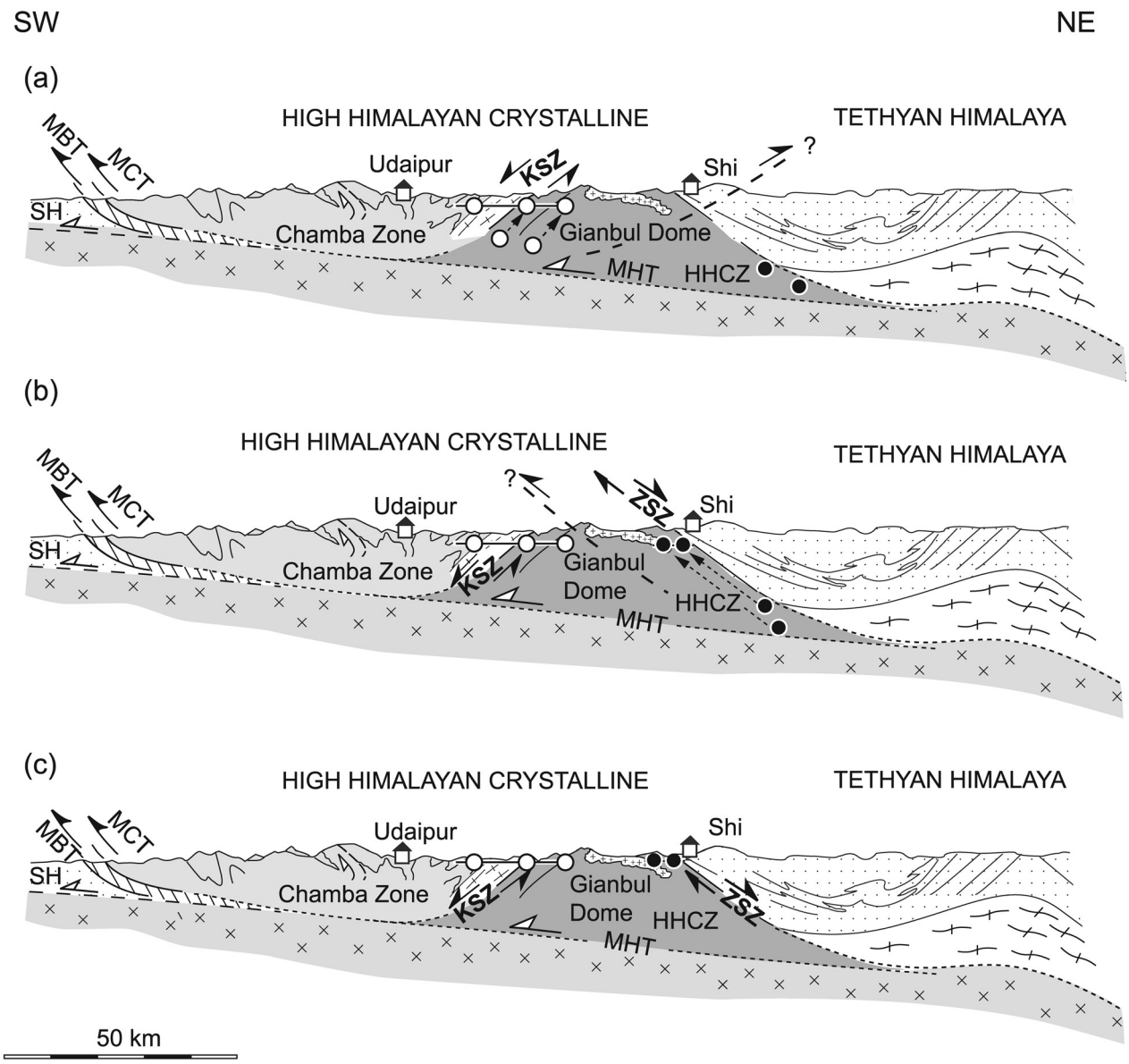

Figure 11. Three kinematic models showing the spatial and temporal relationships between the Khanjar Shear Zone (KSZ) and the Zanskar Shear Zone (ZSZ). An onset of the Khanjar Shear Zone before extensional shearing along the Zanskar Shear zone predicts either (a) a NE directed thrust in the northern part of the transect or (b) a SW directed thrust located between the Zanskar Shear Zone and the Khanjar Shear Zone. (c) The absence of field evidences testifying to the presence of such thrusts suggesting coeval movements along both of these detachments. The black and white dots represent the initial position of the samples a peak metamorphic conditions in the Gianbul Valley and the Miyar Valley, respectively. The dots connected by the black line correspond to the current position of the samples. Abbreviation and symbols are as in Figure 1.

that extension along the KSZ began shortly before 26.6 Ma and ended by 22.56 Ma.

5. Tectonic Implications

[24] Geochronology of various leucogranitic plutons and dikes in the footwall of the ZSZ indicates that the main ductile shearing along that structure occurred between 22.2 Ma and 19.8 Ma [*Dèzes et al.*, 1999]. It thus appears that the KSZ predates the ZSZ. However, this structural evolution does not fit with field observations. Indeed, the exhumation of high-grade metamorphic rocks along the KSZ should have created a major NE directed thrust somewhere farther north to accommodate the extension

along the KSZ (Figure 11a). Such a NE directed thrust is not observed. Yet another problem arises: The samples collected in the Miyar Valley and the Gianbul Valley currently lie at the same elevation (Figure 11c), yet quantitative pressure data indicate a 15 km depth difference between the samples [*Robyr et al.*, 2002]. If ductile shearing along the KSZ predates the extension along the ZSZ, the samples in the Gianbul Valley have to be exhumed along the ZSZ without displacing the sampling line in the Miyar Valley, in order to get a same horizontal sampling line on both sides of the dome. This evolution would imply the formation of a major SW directed thrust zone between the Miyar and the Gianbul Valley (Figure 11b). Again, such a structure is not observed. As a consequence, structural analyses and geometric modeling suggest that the opposite-directed ductile extensional shearing on both sides of the dome, the KSZ and the ZSZ, occurred contemporaneously (Figure 11c). Moreover, the onset of extension along the ZSZ must have begun shortly before 26.6 Ma. This age is in good agreement with data from the northernmost part of the HHCZ of Zanskar, where *Vance and Harris* [1999] suggested a rapid 4 kbar decompression of the HHCZ rocks at circa 25 Ma. In the same area, *Inger* [1998] demonstrated that ductile deformation along the ZSZ was active at 26 Ma. In contrast, 26 Ma is 4 Myr older than the ages from the footwall of the ZSZ. However, this discrepancy is consistent with the interpretation of *Dèzes et al.* [1999], suggesting that their age of 22.2 Ma probably records a late stage of extension.

[25] The record of continuous convergence between India and Eurasia since the onset of the collision indicates that coeval extension along both the ZSZ and the KSZ developed within a compressional orogenic setting. Thus the upper crustal extensional system must have been decoupled from the subsiding lower crust and mantle. As a consequence, the late Oligocene exhumation of high-grade metamorphic rocks in SE Zanskar was likely accompanied by SW directed thrusting at base of the HHC unit. As the structure that underlies the HHC, the MCT is the best candidate for the thrust at the base of the dome. This interpretation is consistent with the different models for the central Himalaya suggesting that the exhumation of the HHC is associated with coeval thrusting along the MCT and extension along the South Tibetan Detachment System [e.g., *Beaumont et al.*, 2001; *Vannay and Grasemann*, 2001, and references therein]. Hence, assuming that the latter models are correct, our new data imply the onset of thrusting along the MCT to start before 26.6 Ma.

6. Synthesis

[26] The petrographic and quantitative P-T results for the Miyar Valley–Gianbul Valley section reveal the depth of burial and thermal structure during the tectonic evolution of the Gianbul dome and the mapping and structural analyses constrain the kinematic evolution. These data, together with the geochronological constraints, enable a new reconstruction of the tectonometamorphic evolution of the Gianbul dome (Figure 12).

[27] At the onset of the India-Asia continental collision during the Eocene (circa 55–50 Ma [*Patriat and Achache*, 1984]), the passive margin of the north Indian plate was covered by a 10–15 km thick sedimentary sequence intruded by Cambro-Ordovician granitic plutons (Figure 12a). The first tectonic event affecting the Indian margin was an early phase of crustal thickening related to NE directed tectonic movements (Figure 12b). This D1 phase most likely took place during the early to middle Eocene, and led to the creation of the Shikar Beh nappe, which was thrust northeastward along the Miyar Thrust [*Steck et al.*, 1993, 1999]. As a consequence of the prograde Barrovian M1 metamorphism induced by this crustal thickening, detrital sediments and granites at the base of the Tethyan Himalaya were transformed into the paragneiss and orthogneiss now forming part of the HHCZ. Beneath the Miyar thrust, the rocks were subducted to ~30 km depth, where temperatures of up to 750–850°C triggered partial melting.

[28] Between the middle Eocene and late Oligocene, a second phase of crustal thickening was related to the SW directed thrusting of the Nyimaling-Tsarap nappe (Figure 12b). The sediments subducted beneath the frontal part of the Nyimaling-Tsarap nappe were transformed into more high-grade HHCZ paragneiss during the prograde Barrovian metamorphism M2 induced by this D2 tectonic phase. Some of these paragneisses were migmatized during subduction, as a consequence of temperatures of up to ~800°C at depths down to ~40 km (Figure 12c)

[29] The activation of the KSZ during the late Oligocene (since ~26.6 Ma) marked the onset of the exhumation of the HHCZ of Zanskar (Figure 12d). Along the Miyar Valley, on the southern limb of the Gianbul dome, the KSZ reactivated the Miyar Thrust and superimposed a second phase of penetrative deformation characterized by extensional asymmetrical shear bands. Geometric modeling strongly suggests that the exhumation of the HHCZ of Zanskar was accompanied by extension along the ZSZ, which reactivated the frontal thrust of the Nyimaling-Tsarap nappe. Rapid synconvergent extension along both of these detachments induced near-isothermal decompression, resulting in an M3 high-T/low-P retrogression of the M1 and M2 prograde metamorphic field gradient.

[30] While the HHCZ of Zanskar was being rapidly exhumed, most of the paragneisses that now form the core of the Gianbul dome were transformed into migmatites by near-isothermal decompression that led to the intrusion of leucogranitic dikes and small plutons during the early Miocene (circa 23–19 Ma; Figure 12e). Following the initial doming phase, further extension along the ZSZ, associated with thrusting along the MCT, led to tectonically controlled extrusion of the HHC toward the south (Figure 12e).

7. Discussion and Conclusions

[31] The peak metamorphic conditions reached in the HHCZ of Zanskar are comparable to what is observed in most sections across the metamorphic core zone all along the range [e.g., *Pêcher*, 1989; *Vannay and Hodges*, 1996;

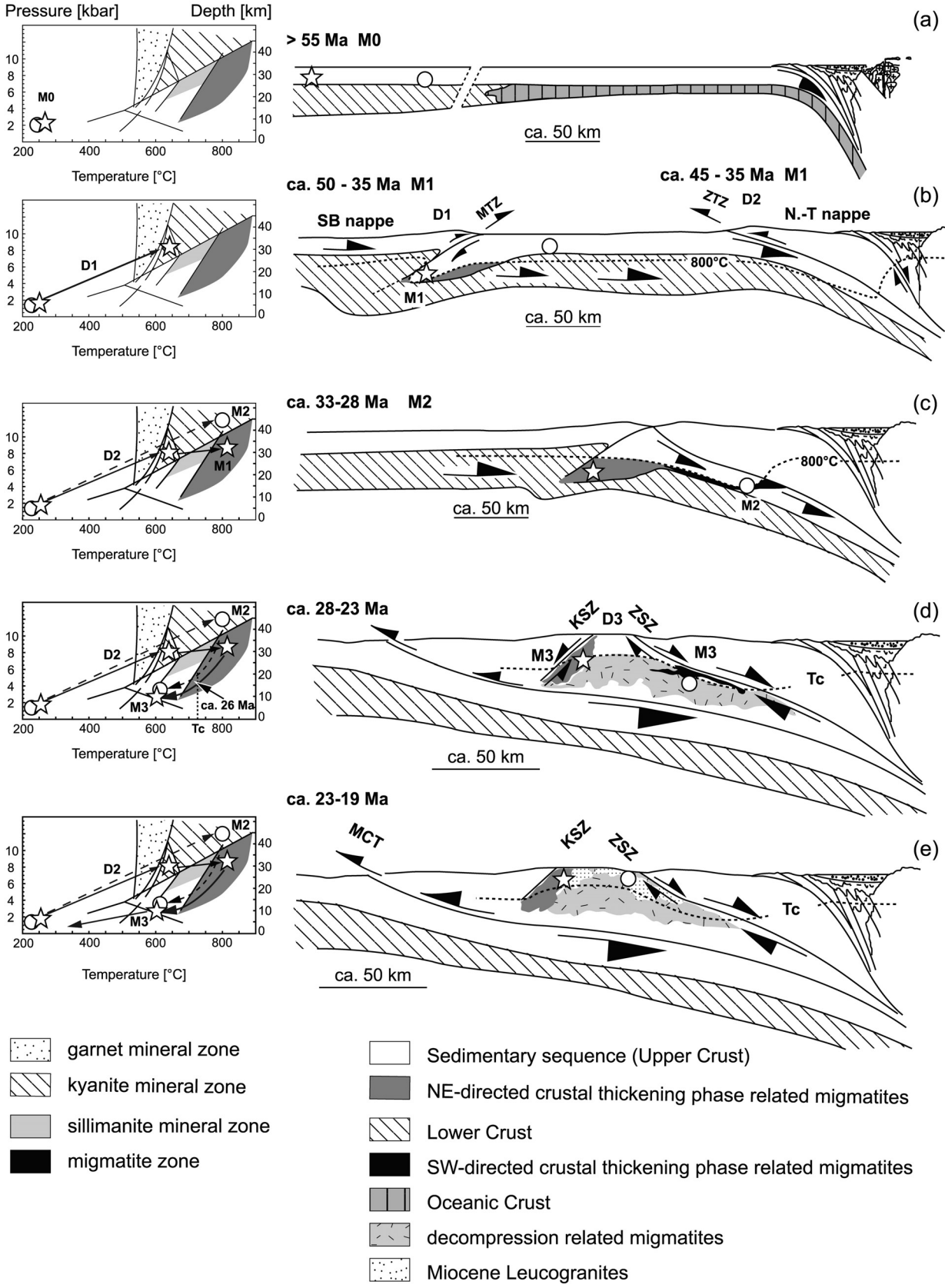
Pressure [kbar]
Depth [km]
Temperature [°C]
M0
D1
D2
M1
M2
M3
ca. 26 Ma
Tc
(a)
> 55 Ma M0
ca. 50 km
(b)
ca. 50 - 35 Ma M1
ca. 45 - 35 Ma M1
SB nappe
D1
MTZ
ZTZ
D2
N.-T nappe
800°C
M1
ca. 50 km
(c)
ca. 33-28 Ma M2
800°C
M2
ca. 50 km
(d)
ca. 28-23 Ma
KSZ
D3
ZSZ
M3
M3
Tc
ca. 50 km
(e)
ca. 23-19 Ma
MCT
KSZ
ZSZ
Tc
ca. 50 km
garnet mineral zone
kyanite mineral zone
sillimanite mineral zone
migmatite zone
Sedimentary sequence (Upper Crust)
NE-directed crustal thickening phase related migmatites
Lower Crust
SW-directed crustal thickening phase related migmatites
Oceanic Crust
decompression related migmatites
Miocene Leucogranites

Figure 12

Dèzes et al., 1999; *Vannay et al.*, 1999; *Wyss*, 2000]. Such P-T results indicate that the HHCZ represents a part of the Indian plate sedimentary cover that was metamorphosed at up to partial melting conditions as a consequence of peak temperatures of ~800°C at depths around 30 km. However, compared to the rest of the belt, the high-grade metamorphic rocks in the NW Indian Himalaya crop out in a more internal part of the orogen as domes, similar to the Himalayan gneiss domes [*Lee et al.*, 2000]. Large-scale doming thus appears to have played a significant role in the exhumation of high-grade rocks in this part of the range, but the origin and emplacement mechanisms of those domes remain debated: various processes such as diapirism, structural interference, ductile thinning and erosion have been invoked. To evaluate these models we consider the following aspects of the structural and metamorphic histories of the Gianbul dome: (1) the burial history of the paragneiss in the HHCZ of Zanskar leading to the development of a significant amount of migmatites in the internal part of the range; (2) the coeval extension along the ZSZ and the KSZ; (3) the P-T-time constraints and duration of extension along both the Khanjar Shear Zone and the ZSZ (from 26.6 Ma to 19.8 Ma); and (4) the overall convergent orogenic setting of the studied area.

[32] The density contrast between the paragneiss that mantles the Tertiary migmatites and leucogranites in the core of the domes has led to proposals that doming could be the consequence of diapirism. Our new data require ~20 km of differential vertical movement across the ZSZ between 26.6 and 22.7 Ma; that is, vertical motion of the HHCZ rocks of the Gianbul Dome took place at an average rate in excess of 5 mm/yr. Recent studies of the ascent and emplacement of granitic magmas suggest that granitic diapirs rise relatively slowly due to viscosity constraints [*Paterson and Vernon*, 1995; *Grocott and Wilson*, 1997; *Clemens et al.*, 1997; *Clemens*, 1998]; a 5-km-thick orthogneiss dome covered by 10 km of metasediments has a calculated rate of diapiric ascent of ~1 mm/yr [*Ramberg*, 1981]. In addition, *Vigneresse and Clemens* [2000] report that the density contrast between magma and surroundings is not sufficient to induce diapirism or fractures and that pluton formation is controlled by local structures rather than by magma properties. Moreover, field evidence from the Gianbul dome indicates that the leucogranites were emplaced by dike propagation [*Dèzes*, 1999], in good agreement with studies suggesting that diapiric ascent of granitic magmas is not a significant mechanism [e.g., *Clemens*, 1998]. As a consequence, although small differences in density are enough for gravitational instability, it seems unlikely that diapirism can account for the rapid exhumation of the HHCZ of Zanskar required by petrology [*Dèzes et al.*, 1999; *Robyr et al.*, 2002].

[33] The superposition of folds can also lead to domal structures if the axial traces of the folds are more or less perpendicular [*Ramsay*, 1962, 1967]. As the Indian Himalaya are strongly controlled by NE-SW compressional tectonics, it is necessary to invoke a significant NW-SE shortening to form a domal interference pattern. Such a superposition of folding appears unlikely given the absence of field structural evidence for significant NW–SE shortening.

[34] Ductile thinning is typically invoked to explain the nearly isothermal decompression observed in many metamorphic core complexes [*Teyssier and Whitney*, 2002]. The geometry, metamorphic zonation, and extensional tectonic contacts characterizing the Himalayan gneiss domes, like the Gianbul dome, are reminiscent of metamorphic core complexes such those in the North American Cordillera [*Vanderhaeghen et al.*, 1999]. This feature suggests that doming could be the consequence of isostatic uplift in the footwall of an extensional detachment. This process results from the gravitational collapse of a previously thickened orogen. Following an initial crustal thickening, thermal relaxation drives a viscosity drop in the lower part of the crust. The isostatic readjustment following the gravitational collapse of the upper crust allows the creep and the rise of the lower crust toward the surface by isostatic compensation, leading to the development of a domal structure in the footwall zone of an extensional detachment. However, in contrast to the metamorphic core complexes that developed during crustal extension, the Himalayan gneiss domes developed during regional shortening and crustal thickening. The similarity between these structures consequently does not imply that they reflect a comparable doming mechanism.

[35] Erosion is another factor which has to be considered in the processes of doming. Although it is a rather slow process of exhumation, erosion cannot be ignored as a permanent factor contributing to the exhumation processes. Moreover, in a mountainous, wet, and tectonically active region like the frontal part of the Himalaya, surficial erosion can locally be very rapid, suggesting a cause and effect relationship between the rate of erosion and the velocity of the exhumation process [*Avouac*, 2003; *Vannay et al.*, 2004, and references therein].

[36] Compared to the central part of the belt, the HHC in the NW part of India are characterized by an earlier phase of metamorphism and tectonics related to NE directed thrusting leading to the creation of a SW dipping major thrust zone (the Miyar Thrust Zone). This feature seems to have had a major influence on the tectonothermal evolution of the HHC of NW India by generating first a weak zone in the upper crust and second a significant amount of low-density and low-viscosity migmatitic rocks in the footwall of the Miyar Thrust Zone. Numerical modeling of channel flow predicts that the extrusion location of high-grade rocks is controlled by two significant parameters: (1) the erosion rate at the orogenic front and (2) the strength of the upper crust

Figure 12. Kinematic model for the exhumation history of the Gianbul dome, based on P-T results, structural data and geochronological constraints. SB nappe, Shikar Beh nappe; N-T Nappe, Nyimaling-Tsarap nappe; MTZ, Miyar Thrust Zone; ZTZ, Zanskar Thrust Zone; KSZ, Khanjar Shear Zone; ZSZ, Zanskar Shear Zone.

[*Beaumont et al.*, 2001]: efficient erosion and a strong upper crust induce extrusion in the frontal part of the range, such as observed in most of the studied Himalayan sections, whereas reduced erosion and a weak upper crust can lead to extrusion in a more internal part of the range. This latter scenario appears consistent, to first order, with the NW Himalaya where high-grade metamorphic rocks were exhumed in the internal part of the range. In addition, the close spatial coincidence between active exhumation of deep crustal rocks and vigorous fluvial erosion highlights the major influence that geomorphic processes may have had on the deep tectonometamorphic evolution during the Himalayan orogeny [*Vannay et al.*, 2004]. According to these studies, the lack of high-grade metamorphic rocks in the hanging wall of the frontal MCT between the Kulu Valley and the downstream part of the Chenab Valley strongly suggest reduced erosion in this region, possibly because of a lack of major rivers in the Chamba area (Figure 1). As a consequence, the weakness generated in the upper crust by the presence of two major converging thrust zones (the Miyar Thrust Zone and the Zanskar Thrust), associated with the geomorphic characteristic of the Chamba zone, could have forced the tectonic extrusion of the high-grade metamorphic rocks of the HHCZ of Zanskar in a more internal part of the Himalayan orogen. Taken into account these various models, the density contrast, the geomorphic and tectonic features, and the P-T-time data for the studied area, the following scenario can be proposed for the mechanism of the Gianbul dome formation.

[37] During the two first opposite-directed crustal thickening phases, the high-grade rocks of the HHC of Zanskar were buried to 30 km depth, where temperatures up to 850°C triggered partial melting. The relatively high buoyancy of these low-density and low-viscosity migmatites counteracted the downward force exerted by the still subsiding lithosphere. From that moment, the migmatitic rocks of the HHC of Zanskar were caught between the Indian plate and the backstop formed by the north Himalayan nappe stack (Nyimaling-Tsarap nappe) of the Tethyan Himalaya. The presence of two major thrust zones directly above this migmatitic zone induced a weakness in the upper crust that facilitated the exhumation of these high-grade, low-viscosity migmatites. Once the onset of extension along this detachment was triggered, decompression drove partial melting, leading to positive feedback between melting and decompression that enhanced exhumation. Further extension along the ZSZ associated with combined thrusting along the MCT led to the further extrusion of the HHC toward the south.

[38] Our model thus implies that ductile exhumation of these high-grade, low-viscosity paragneiss and migmatites was controlled by gravity forcing and underthrusting of the Indian plate. Compared to the central and eastern part of the belt where crustal shortening is mainly accommodated by foreland-directed extrusion of high-grade rocks, the large-scale domes of the NW Himalaya could result from subvertical ductile extrusion of high-grade metamorphic rocks as the consequence of interaction between erosion and tectonothermal evolution. As a consequence, the doming of high-grade metamorphic rocks could reflect an alternative way that the Himalaya has accommodated crustal shortening in a compressional orogenic setting.

[39] **Acknowledgments.** This study was carried out during a postdoctoral visit of the first author to UCSB, financed by a research grant from the Swiss National Fund for Scientific Research (FNSR) and the U.S. National Science Foundation (EAR-0003568). Fieldwork in Zanskar was financed by the Swiss National Fund for Scientific Research (FNRS grant 2000-067037.01). The analytical expenses were provided by grants from the Société Académique Vaudoise. We are grateful to M. Grove for supervising SIMS analyses at UCLA, to M. Rioux for assisting with sample preparation and SIMS analyses. Highly constructive discussions and comments by J.-L. Epard, A. Steck, J.-C. Vannay, and T. Mueller significantly improved this manuscript. M. Hubbard and an anonymous reviewer provided helpful comments. Special thanks to all the people of the Department of Earth Sciences at UCSB, who contributed to make the stay of the first author pleasant.

References

Avouac, J.-P. (2003), Mountain building, erosion, and the seismic cycle in the Nepal Himalaya, *Adv. Geophys.*, *46*, 1–80.

Ayers, J. C., C. Miller, B. Gorisch, and J. Milleman (1999), Textural development of monazite during high-grade metamorphism: Hydrothermal growth kinetics, with implications for U, Th-Pb geochronology, *Am. Mineral.*, *84*, 1766–1780.

Beaumont, C., R. A. Jamieson, M. H. Nguyen, and B. Lee (2001), Himalayan tectonics explained by extrusion of a low-viscosity crustal channel coupled to focused surface denudation, *Nature*, *414*, 738–742.

Bonhomme, M., and E. Garzanti (1991), Age of metamorphism in the Zanskar Tethys Himalaya (India), *Geol. Alpine*, *16*, 15–16.

Braun, I., J.-M. Montel, and C. Nicollet (1998), Electron microprobe dating of monazites from high-grade gneisses and pegmatites of the Kerala khondalite belt, southern India, *Chem. Geol.*, *146*, 65–85.

Burchfiel, B. C., Z. Chen, K. V. Hodges, Y. Liu, L. H. Royden, C. Deng, and J. Xu (1992), The South Tibetan Detachment System, Himalayan orogen: Extension contemporaneous with and parallel to shortening in a collisional mountain belt, *Spec. Pap. Geol. Soc. Am.*, *269*, 41 pp.

Catlos, E. J., L. D. Gilley, and T. M. Harrison (2002), Interpretation of monazite ages obtained via in situ analysis, *Chem. Geol.*, *188*, 193–215.

Cherniak, D. J., E. B. Watson, M. Grove, and T. M. Harrison (2004), Pb diffusion in monazite: A combined RBS/SIMS study, *Geochim. Cosmochim. Acta*, *68*, 829–840.

Clemens, J. D. (1998), Observations on the origins and ascent mechanisms of granitic magmas, *J. Geol. Soc. London*, *155*, 843–851.

Clemens, J. D., N. Petford, and C. K. Mawer (1997), Ascent mechanisms of granitic magmas: Causes and consequences, in *Deformation-Enhanced Fluid Transport in the Earth's Crust and Mantle*, edited by M. B. Holness, pp. 144–171, CRC Press, Boca Raton, Fla.

Coleman, M. E. (1998), U-Pb constraints on Oligocene-Miocene deformation and anatexis within the central Himalaya, Marsyandi valley, Nepal, *Am. J. Sci.*, *298*, 553–571.

Copeland, P., R. R. Parrish, and T. M. Harrison (1988), Identification of inherited radiogenic Pb in monazite and its implications, *Nature*, *333*, 760–763.

Dèzes, P. (1999), *Tectonic and Metamorphic Evolution of the Central Himalayan Domain in Southeast Zanskar (Kashmir, India)*, *Mém. Géol., 32*, 149 pp., Univ. of Lausanne, Lausanne, Switzerland.

Dèzes, P., J.-C. Vannay, A. Steck, F. Bussy, and M. Cosca (1999), Synorogenic extension: Quantitative constraints on the age and displacement of the Zanskar Shear Zone (NW Himalayas), *Geol. Soc. Am. Bull.*, *111*, 364–374.

Epard, J.-L., and A. Steck (2004), The eastern prolongation of the Zanskar Shear Zone (western Himalaya), *Eclogae Geol. Helv.*, *97*, 193–212.

Epard, J.-L., A. Steck, J.-C. Vannay, and J. Hunziker (1995), Tertiary Himalayan structures and metamorphism in the Kulu Valley (Mandi-Khoksar transect of the western Himalaya)–Shikar Beh Nappe and Crystalline Nappe, *Schweiz. Mineral. Petrogr. Mitt.*, *75*, 59–84.

Fitzsimons, I. C. W., P. D. Kinny, and S. L. Harley (1997), Two stages of zircon and monazite growth

in anatectic leucogneiss: SHRIMP constraints on the duration and intensity of Pan-African metamorphism in Prydz Bay, East Antarctica, *Terra Nova*, *9*, 47–51.

Foster, G., P. Kinny, D. Vance, C. Prince, and N. Harris (2000), The significance of monazite U-Th-Pb age data in metamorphic assemblages: A combined study of monazite and garnet chronometry, *Earth Planet. Sci. Lett.*, *181*, 327–340.

Frank, W., M. Thoni, and F. Purtscheller (1977), Geology and petrography of Kulu - South Lahul area, *Colloq. Int. Cent. Natl. Rech. Sci.*, *268*, 147–172.

Garzanti, E., A. Baud, and G. Mascle (1987), Sedimentary record of the northward flight of India and its collision with Eurasia (Ladakh Himalaya, India), *Geodin. Acta*, *1*, 297–312.

Grocott, J., and J. Wilson (1997), Ascent and emplacement of granitic plutonic complexes in subduction-related extensional environments, in *Deformation-Enhanced Fluid Transport in the Earth's Crust and Mantle*, edited by M. B. Holness, pp. 173–195, CRC Press, Boca Raton, Fla.

Guillot, S., K. V. Hodges, P. Le Fort, and A. Pêcher (1994), New constraints on the age of the Manaslu Leucogranite: Evidence for episodic tectonic denudation in the central Himalayas, *Geology*, *22*, 21–43.

Harrison, T. M., K. D. Mc Keegan, and P. Le Fort (1995), Detection of inherited monazite in the Manaslu leucogranite by $^{208}Pb/^{232}Th$ ion microprobe dating: Crystallization age and tectonic implications, *Earth Planet. Sci. Lett.*, *133*, 271–282.

Harrison, T. M., M. Grove, K. D. Mc Keegan, C. D. Coath, O. M. Lovera, and P. Le Fort (1999), Origin and episodic emplacement of the Manaslu Intrusive Complex, central Himalaya, *J. Petrol.*, *40*, 3–9.

Harrison, T. M., E. J. Catlos, and J.-M. Montel (2002), U-Th-Pb dating of phosphate minerals, in *Phosphates: Geochemical, Geobiological, and Materials Importance*, *Rev. Mineral. Geochem.*, vol. 48, edited by M. J. Kohn, J. Rakovan, and J. Hughes, pp. 523–558, Mineral. Soc. Am., Washington, D. C.

Hawkins, D. P., and S. A. Bowring (1997), U-Pb systematics of monazite and xenotime: Case studies from the Paleoproterozoic of the Grand Canyon, Arizona, *Contrib Mineral. Petrol.*, *127*, 87–103.

Hawkins, D. P., and S. A. Bowring (1999), U-Pb monazite, xenotime and titanite geochronological constraints on the prograde to post-peak metamorphic thermal history of Paleoproterozoic migmatites from the Grand Canyon, Arizona, *Contrib Mineral. Petrol.*, *134*, 150–169.

Herren, E. (1987), Northeast-southwest extension within the Higher Himalayas (Ladakh, India), *Geology*, *15*, 409–413.

Hodges, K. V. (2000), Tectonics of the Himalaya and southern Tibet from two perspectives, *Geol. Soc. Am. Bull.*, *112*, 324–350.

Hodges, K. V., R. R. Parrish, T. B. Housh, D. R. Lux, B. C. Burchfiel, L. H. Royden, and Z. Chen (1992), Simultaneous Miocene extension and shortening, *Science*, *258*, 1466–1469.

Hodges, K. V., R. R. Parrish, and M. P. Searle (1996), Tectonic evolution of the central Annapurna Range, Nepalese Himalayas, *Tectonics*, *15*, 1264–1291.

Honegger, K., V. Dietrich, W. Frank, A. Gansser, M. Thoeni, and V. Trommsdorff (1982), Magmatism and metamorphism in the Ladakh Himalayas (the Indus-Tsangpo suture zone), *Earth Planet. Sci. Lett.*, *60*, 253–292.

Hubbard, M. S., and T. M. Harrison (1989), $^{40}Ar/^{39}Ar$ age constraints on deformation and metamorphism in the Main Central Thrust Zone and Tibetan Slab, eastern Nepal Himalaya, *Tectonics*, *8*, 865–880.

Inger, S. (1998), Timing of an extensional detachment during convergent orogeny: New Rb-Sr geochronological data from the Zanskar Shear Zone, northwestern Himalaya, *Geology*, *26*, 223–226.

Jaffey, A. H., K. F. Flynn, L. E. Glendenin, W. C. Bentley, and A. M. Essling (1971), Precision measurement of half-lives and specific activities of ^{235}U and ^{238}U, *Phys. Rev. C*, *4*, 1889–1906.

Janda, C., C. Hager, B. Grasemann, E. Draganits, J.-C. Vannay, B. Bookhagen, and R. Thiede (2002), The Karcham Normal Fault: Implications for an active extruding wedge, Sutlej Valley, NW Himalaya, *J. Asian Earth Sci.*, *20*, 19–20.

Kamber, B. S., R. Frei, and A. J. Gibb (1998), Pitfalls and new approaches in granulite chronometry; an example from the Limpopo Belt, Zimbabwe, *Precambrian Res.*, *91*, 269–285.

Kündig, R. (1989), Domal structures and high-grade metamorphism in the Higher Himalayan Crystalline, Zanskar Region, north-west Himalaya, India, *J. Metamorph. Geol.*, *7*, 43–55.

Lanzirotti, A., and G. N. Hanson (1996), Geochronology and geochemistry of multiple generations of monazite from the Wepawaug Schist, Connecticut, USA: Implications for monazite stability in metamorphic rocks, *Contrib Mineral. Petrol.*, *125*, 332–340.

Lee, J., B. R. Hacker, W. S. Dinklage, P. B. Gans, A. Calvert, Y. Wang, J. Wan, and W. Chen (2000), Evolution of the Kangmar Dome, southern Tibet: Structural, petrologic, and thermochronologic constraints, *Tectonics*, *19*, 872–895.

Molnar, P., and P. Tapponier (1975), Cenozoic tectonics of Asia: Effects of a continental collision, *Science*, *189*, 419–426.

Parrish, R. R. (1990), U-Pb dating of monazite and its application to geological problems, *Can. J. Earth Sci.*, *27*, 1431–1450.

Patel, R. C., S. Singh, A. Asokan, R. M. Manickavasagam, and A. K. Jain (1993), Extensional tectonics in the Himalayan Orogen, Zanskar, NW India, in *Himalayan Tectonics*, edited by P. J. Treolar and M. P. Searle, *Geol. Soc. Spec. Publ.*, *74*, 445–459.

Paterson, S. R., and R. H. Vernon (1995), Bursting the bubble of ballooning plutons: A return to nested diapirs emplaced by multiple processes, *Geol. Soc. Am. Bull.*, *107*, 1356–1380.

Patiño-Douce, A. E., and N. Harris (1998), Experimental constraints on Himalayan anatexis, *J. Petrol.*, *39*, 689–710.

Patriat, P., and J. Achache (1984), India-Eurasia collision chronology has implications for crustal shortening and driving mechanism of plates, *Nature*, *311*, 615–621.

Pêcher, A. (1989), The metamorphism in the central Himalaya, in *Himalayan Metamorphism*, edited by A. C. Barnicoat and P. J. Treloar, *J. Metamorph. Geol.*, *7*, 31–41.

Pognante, U., D. Castelli, P. Benna, G. Genovese, F. Oberli, M. Meier, and M. Tonarini (1990), The crystalline units of the High Himalayas in the Lahul Zanskar region (northwest India): Metamorphic-tectonic history and geochronology of the collided and imbricated India plate, *Geol. Mag.*, *127*, 101–116.

Poitrasson, F., F. Chenery, and D. Bland (1996), Contrasted monazite hydrothermal alteration mechanisms and their geochemical implications, *Earth Planet. Sci. Lett.*, *145*, 79–96.

Pyle, J. M., F. S. Spear, R. L. Rudnick, and W. F. McDonough (2001), Monazite-xenotime-garnet equilibrium in metapelites and a new monazite-garnet thermometer, *J. Petrol.*, *42*, 2083–2107.

Ramberg, H. (1981), The role of gravity in orogenic belts, in *Thrust and Nappe Tectonics*, edited by K. R. McClay and N. J. Price, *Geol. Soc. Spec. Publ.*, *9*, 125–140.

Ramsay, J. G. (1962), The geometry and mechanics of formation of "similar" type folds, *J. Geol.*, *70*, 309–327.

Ramsay, J. G. (1967), *Folding and Fracturing of Rocks*, 568 pp. McGraw-Hill, New York.

Robyr, M. (2002), *Thrusting, Extension and Doming in the High Himalaya of Lahul Zanskar Area (NW India): Structural and Pressure-Temperature Constraints*, *Mém. Géol., 32*, 127 pp., Univ. of Lausanne, Lausanne, Switzerland.

Robyr, M., J.-C. Vannay, J.-L. Epard, and A. Steck (2002), Thrusting, extension and doming during the polyphase tectonometamorphic evolution of the High Himalayan Crystalline Zone in NW India, *J. Asian Earth Sci.*, *21*, 221–239.

Rowley, D. B. (1996), Age of initiation of collision between India and Asia: A review of stratigraphic data, *Earth Planet. Sci. Lett.*, *145*, 1–13.

Rubatto, D., I. S. Williams, and I. S. Buick (2001), Zircon and monazite response to prograde metamorphism in the Reynolds Range, central Australia, *Contrib Mineral. Petrol.*, *140*, 458–468.

Schlup, M., A. Carter, M. Cosca, and A. Steck (2003), Exhumation history of eastern Ladakh revealed by $^{40}Ar/^{39}Ar$ and fission-track ages: The Indus River–Tso Morari transect, NW Himalaya, *J. Geol. Soc. London*, *160*, 385–399.

Searle, M. P., D. J. Waters, M. W. Dransfield, B. J. Stephenson, C. B. Walker, J. D. Walker, and D. C. Rex (1999), Thermal and mechanical models for the structural and metamorphic evolution of the Zanskar High Himalaya, in *Continental Tectonics*, edited by C. Mac Niocaill and P. D. Ryan, *Geol. Soc. Spec. Publ.*, *164*, 139–156.

Smith, H. A., and B. Giletti (1997), Lead diffusion in monazite, *Geochim. Cosmochim Acta*, *61*, 1047–1055.

Spear, F., M. J. Kohn, and J. T. Cheney (1999), P-T paths from anatectic pelites, *Contrib. Mineral. Petrol.*, *134*, 17–32.

Stäubli, A. (1989), Polyphase metamorphism and the development of the Main Central Thrust, *J. Metamorph. Geol.*, *7*, 73–93.

Steck, A. (2003), Geology of the NW Indian Himalaya, *Eclogae Geol. Helv.*, *96*, 147–196.

Steck, A., L. Spring, J.-C. Vannay, H. Masson, H. Bucher, E. Stutz, R. Marchant, and J.-C. Tièche (1993), The tectonic evolution of the northwestern Himalaya in eastern Ladakh and Lahul, India, in *Himalayan Tectonics*, edited by P. J. Treloar and M. P. Searle, *Geol. Soc. Spec. Publ.*, *74*, 264–276.

Steck, A., J.-L. Epard, J.-C. Vannay, J. Hunziker, M. Girard, A. Morard, and M. Robyr (1998), Geological transect across the Tso Morari and Spiti areas: The nappe structures of the Tethys Himalaya, *Eclogae Geol. Helv.*, *91*, 103–122.

Steck, A., J.-L. Epard, and M. Robyr (1999), The NE-directed Shikar Beh Nappe: A major structure of the Higher Himalaya, *Eclogae Geol. Helv.*, *92*, 239–250.

Stephenson, B. J., D. J. Waters, and M. P. Searle (2000), Inverted metamorphism and the Main Central Thrust: Field relations and thermobarometric constraints from the Kishtwar Window, NW Indian Himalaya, *J. Metamorph. Geol.*, *18*, 571–590.

Suzuki, K., M. Adachi, and I. Kajizuka (1994), Electron microprobe observations of Pb diffusion in metamorphosed detrital monazites, *Earth Planet. Sci. Lett.*, *128*, 391–405.

Teyssier, C., and L. D. Whitney (2002), Gneiss dome and orogeny, *Geology*, *30*, 1139–1142.

Thakur, V. C. (1998), Structure of the Chamba nappe and position of the Main Central Thrust in Kashmir Himalaya, *J. Asian Earth Sci.*, *16*, 269–282.

Townsend, K. J., C. F. Miller, J. L. D'Andrea, J. C. Ayers, T. M. Harrison, and C. D. Coath (2001), Low temperature replacement of monazite in the Ireteba granite, southern Nevada: Geochronological implications, *Chem. Geol.*, *172*, 95–112.

Vance, D., and N. Harris (1999), Timing of prograde metamorphism in the Zanskar Himalaya, *Geology*, *27*, 395–398.

Vanderhaeghen, O., J.-P. Burg, and C. Teyssier (1999), Exhumation of migmatites in two collapsed orogens: Canadian Cordillera and French Variscides, in *Exhumation Processes: Normal faulting, Ductile Flow and Erosion*, edited by. U. Ring, M. T. Brandon, G. S. Lister, and S. D. Willett, *Geol. Soc. London*, *154*, 181–204.

Vannay, J.-C. (1993), *Géologie des Chaines du Haut-Himalaya et du Pir Panjal au Haut-Lahul (NW Himalaya, Inde): Paleogeographie et Tectonique*, *Mém. Géol., 16*, 148 pp., Univ. of Lausanne, Lausanne, Switzerland.

Vannay, J.-C., and B. Grasemann (2001), Himalayan inverted metamorphism and syn-convergence extension as a consequence of a general shear extrusion, *Geol. Mag.*, *138*, 253–276.

Vannay, J.-C., and K. V. Hodges (1996), Tectonometamorphic evolution of the Himalayan metamorphic core between the Annapurna and Dhaulagiri, central Nepal, *J. Metamorph. Geol.*, *14*, 635–656.

Vannay, J.-C., and A. Steck (1995), Tectonic evolution of the High Himalaya in Upper Lahul (NW Himalaya, India), *Tectonics*, *14*, 253–263.

Vannay, J.-C., Z. D. Sharp, and B. Grasemann (1999), Himalayan inverted metamorphism constrained by oxygen isotope thermometry, *Contrib. Mineral. Petrol.*, *137*, 90–101.

Vannay, J.-C., B. Grasemann, M. Rahn, W. Frank, A. Carter, V. Baudraz, and M. Cosca (2004), Miocene to Holocene exhumation of metamorphic crustal wedges in the NW Himalaya: Evidence for tectonic extrusion coupled to fluvial erosion, *Tectonics*, *23*, TC1014, doi:10.1029/2002TC001429.

Vigneresse, J. L., and J. D. Clemens (2000), Granitic magma ascent and emplacement: Neither diapirism nor neutral buoyancy, in *From the Arctic to the Mediterranean: Salt, Shale and Igneous Diapirs in and Around Europe*, edited by B. Vendeville, Y. Mart, and J. L. Vigneresse, *Geol. Soc. Spec. Publ.*, *174*, 1–19.

Walker, J. D., M. W. Martin, S. A. Bowring, M. P. Searle, D. J. Waters, and K. V. Hodges (1999), Metamorphism, melting, and extension: Age constraints from the High Himalayan Slab of southeast Zanskar and northwest Lahul, *J. Geol.*, *107*, 473–495.

Wiesmayr, G., and B. Grasemann (1999), Balanced cross-section and depth-to-detachment calculations for the Tethyan Himalaya (Spiti, N India): Where is the crystalline basement of the Higher Himalaya?, *J. Conf. Abstr.*, *4*(1), 51.

Wyss, M. (2000), Metamorphic evolution of the northern Himachal Himalaya: Phase equilibria constraints and thermobarometry, *Schweiz. Mineral. Petrogr. Mitt.*, *80*, 317–350.

Wyss, M., J. Hermann, and A. Steck (1999), Structural and metamorphic evolution of the northern Himachal Himalaya, NW India (Spiti-eastern Lahul-Parvati valley traverse), *Eclogae Geol. Helv.*, *92*, 3–44.

Yin, A., and T. M. Harrison (2000), Geologic evolution of the Himalayan-Tibetan Orogen, *Annu. Rev. Earth Planet. Sci.*, *28*, 211–280.

B. R. Hacker and J. M. Mattinson, Geological Sciences, University of California, Santa Barbara, CA 93106-9630, USA.

M. Robyr, Institut de Minéralogie et Géochimie, Université de Lausanne, CH-1015 Lausanne, Switzerland. (martin.robyr@unil.ch)